AMEGHINIANA
A GONDWANAN PALEONTOLOGICAL JOURNAL



contained in this volume are to be published in future issues of the journal.
Please be aware that during the production process errors may be discovered which could affect the content.
All legal disclaimers that apply to the journal pertain.

Submitted: August 22th, 2019 – **Accepted**: May 15th, 2020 – **Published online**: May 23th, 2020

To link and cite this article:

doi: https://doi.org/10.5710/AMGH.15.05.2020.3285

PLEASE SCROLL DOWN FOR ARTICLE

Passive-dynamic walkers of the late Paleozoic

ALEXANDER N. KUZNETSOV

Borissiak Paleontological Institute, Russian Academy of Sciences, Moscow, 117647, Russia

Email: sasakuzn@mail.ru

Key words: Pareiasauria, *Sukhonopus*, trackway, gait analysis, glenoacetabular length, pace-like walk, reverse engineering

ABSTRACT — Two upper Permian trackways attributed to the ichnogenus *Sukhonopus*, which were originally interpreted as produced by pareiasaurians, have been studied. Based on the statistical analysis of dimensions of the longer trackway representing 15.5 locomotor cycles, the *Sukhonopus* gait was defined as a lateral-sequence walk shifted by ipsilateral limb synchronization towards the slow pace. This conclusion gained additional support through comparison of dimensions of the two trackways with the glenoacetabular-to-pes length ratio measured on the skeletons of the pareiasaur *Deltavjatia*. With the sprawling limb posture typical to lower tetrapods, including pareiasaurians, the pace can be only performed with body rocking from side to side, according to the principles of passive-dynamic walking. A natural-sized (185 cm long) model of the *Sukhonopus* producer was built. This model reproduces the passive-dynamic rocking pace, being driven manually by children pulling it forward by the rope and simultaneously pushing it from side to side. The passive-dynamic rocking pace of pareiasaurs, proved to be feasible by the model, requires functional differentiation of the hindlimbs and the forelimbs. The former were more appropriate for propulsion, while the latter were more efficient in generation of the transverse forces required to pump the rocking motion. It is hypothesized that this walking mechanism was associated with archaic deficiency of nervous and muscular supply of the limbs. Possibly, it was also

employed by some other Paleozoic tetrapods. The ichnological evidence of this locomotion technique is the inward turn of the forelimb footprints, and the histological evidence is the extensive development in the long limb elements of spongy bone tissue in place of the superficial compact bone layer and marrow cavity.

INTRODUCTION

How far is a paleontologist, who undertakes to reconstruct the locomotion techniques and gaits of extinct animals, allowed to go beyond constraints known for extant animals? Is it possible to test that iconic *Ichthyostega* moved on land by "inchworm shuffling" like a seal (Ahlberg *et al*., 2005), or that *Edmontosaurus* dinosaur galloped like quadrupedal mammals or hopped like kangaroos (Sellers *et al*., 2009)? Even ichnofossils, which are direct evidence of activity, are often misleading. For instance, fossilized imprints that seemed to be the footprints of a giant super-ancient *Ichthyostega* and bilaterally-symmetrical trackways of smaller tetrapodomorphs (Niedźwiedzki *et al*., 2010) appear to be fish nests or feeding pits according to more recent interpretations (Lucas, 2015). Also, a fossilized imprint that seemed to be the footprint of *Eusthenopteron* (Gregory, 1951), which was treated as the closest model of tetrapod ancestor in the 20th century before discovery of *Tiktaalik* (Daeschler, 2006), was subsequently re-interpreted as a fossilized fish coprolite (Lucas, 2015). Even for a perfectly preserved trackway, it is sometimes problematic to determine confidently its fore-and-aft polarity, that is, the direction of animal movement (Warren & Wakefield, 1972; Clack, 1997). Most confusing is that the gait identification is problematic if the body size and proportions of the trackmaker are unknown (Peabody, 1959; Kienapfel *et al*., 2014). So, the basic question "Who was the trackmaker?" should be better solved before "How did it walk?", because this "How" very much depends on that "Who" through the knowledge of body structure and proportions.

In this study, the biomechanics of a possible producer of the upper Permian ichnotaxon *Sukhonopus* was modeled. Originally, it was described by Gubin *et al*. (2003) as a pareiasaurian trackway. This interpretation was later supported by Valentini *et al*. (2009), who suggested to synonymize the ichnogenera *Sukhonopus* and *Pachypes* retaining the latter as the senior one by priority. Even later (Marchetti *et al*., 2017), *Sukhonopus*, among other large Permian tetrapod footprints from Russia, were said to be poorly preserved regarding ichnotaxonomically relevant features. The purpose of the current research is not to thoroughly re-describe the available *Sukhonopus* specimens in search for new morphological features thereof, which could be ichnotaxonomically relevant and could support or reject the ascription of these trackways to a pareiasaurian. Contrary to that, the purpose is to reconstruct the locomotion technique of the trackmaker and consider whether it was plausible in pareiasaurians. Plausibility of the reconstruction have been tested by a reverse-engineering of the natural-sized walking model with pareiasaurian body proportions. The required mechanical properties of the limb skeleton have been tested against pareiasaurian bone histology which was recently discovered (Canoville & Chinsamy, 2017; Boitsova *et al*., 2019).

To introduce the trackway analysis, an excerpt from the theory of gaits is required. The general pattern of the trackways under study, as well as of those of the majority of lower tetrapods, is the same as in human trackways although the former were produced by a quadruped. This pattern is known as the uniform glide-reflection symmetry (Lee & Liu, 2012). It means that the left part of the trackway is equal to the mirror reflection of the right half over the trackway midline, shifted forward or backward by one-step length, and vice versa. The uniformity of this pattern is based on an anti-phase movement of the two contralateral limbs of the same pair. For instance, when the left forelimb is maximally protracted going to touch the ground, the right one is maximally retracted, and vice versa, and

the same is true for the hindlimbs. This comes from bilateral symmetry of the body, and the gaits, which keep this anti-phase rule, are known as symmetrical gaits (Howell, 1944). This counter-movement of the two limbs in a pair is the major constraint of symmetrical gaits, whose direct consequence is that the footfall of any chosen limb inevitably falls somewhere in the time interval between the footfalls of the two limbs of the other pair. The resultant footfall sequence has a general form as follows: reference limb – first limb of the other pair – mirror limb for the reference one – second limb of the other pair – reference limb again – etc. In fact, the sequence is completely defined by the first two limbs, because the next two are bilaterally symmetrical to the first ones, and then the cycle is repeated. There are only two variants: reference limb – diagonal limb – mirror and reference limb – ipsilateral limb – mirror. These two quadrupedal sequences are known as symmetrical sequences and they correspond to all variety of symmetrical gaits from trot characterized by the zero time interval between footfalls of the reference limb and the diagonal limb and pace characterized by the zero time interval between footfalls of the reference limb and the ipsilateral limb. However, in symmetrical gait definition there remains an important, though technical problem: which limb to choose as the reference one for the locomotor cycle? Choosing the forelimb, *e.g.*, the right one, as Gray (1944) did, followed by Sukhanov (1963, 1967, 1968, 1974), one comes to the diagonal sequence (right fore – left hind – mirror) and the lateral sequence (right fore – right hind – mirror). Choosing the hindlimb, as Hildebrand (1965, 1966, 1967, 1968) did, followed by the majority of gait researchers, one comes to the diagonal sequence (right hind – left fore – mirror) and the lateral sequence (right hind – right for – mirror). The problem is that in the complete locomotor cycle, the forelimb-based diagonal definition corresponds to the hindlimb-based lateral one, and vice versa. The hindlimb-based notion is newer and is now generally accepted; therefore, it will be used herein too, although it would be more correct to restore the priority of the forelimb-based definition as it is done in taxonomy. In

any case, the diagonal sequence and the lateral sequence refer to the order of the limb motions (*e.g.*, footfalls), and should not be mixed with overlaps in their action, such as the diagonal support (most pronounced in but not restricted to trot) and the lateral support (most pronounced in but not restricted to pace).

Beyond the scope of this study are asymmetrical gaits opposed to the symmetrical ones (Howell, 1944). They need a brief comment to clarify the counter-intuitive terminology. The point is that the symmetrical gaits produce trackways whose symmetry is glide-reflection over the midline, while the asymmetrical gaits can produce both asymmetrical and truly bilaterally symmetrical trackways. Generally, the asymmetrical gaits' variety is much greater than that of the symmetrical gaits (Hildebrand, 1977). The major difference is that in the asymmetrical gaits, the bilaterally symmetrical limbs in a pair do not move in strict anti-phase. The shift towards in-phase action is mutually independent in the fore- and the hindlimb pairs, but is large enough to ensure their coupled instead of alternating action like reference limb – mirror limb – first limb of the other pair – second limb of the other pair – reference limb again – etc. The general name for all asymmetrical quadrupedal gaits is "gallop". One of the most deviating from the anti-phase limb action of the symmetrical gaits is the gallop with in-phase action of the forelimbs followed by in-phase action of the hindlimbs. This gait is termed "bound"; it can be seen in a squirrel and, in spite of its attribution to the asymmetrical gaits, it produces trackways whose symmetry is truly bilateral. It is the left-right reflection alone, in contrast to the glide-reflection symmetry of the trackways of symmetrical gaits where the step-long translation is added to reflection. The contradiction between the asymmetrical nature of the bound as a gait and the bilateral symmetry of its trackways often leads to confusion in ichnological studies. Fore instance, in Niedźwiedzki *et al*. (2010, Supplementary material therein), the seemingly bilaterally symmetrical pit rows are treated either as "parallel gait" or as "symmetrical gait"

(Supplementary material, Fig. 12 therein) of the earliest tetrapods. The first term is non-existent, the second one is incorrectly applied. In addition, as was noted above, these traces appear to be not tetrapod trackways but fish nests or feeding pits (Lucas, 2015).

Returning to interpretation of the true symmetrical gait trackways, one more difficult problem should be taken into account, which is by now underestimated. The problem is how to distinguish, based on the glide-reflection symmetrical trackway, where was the trackmaker's gait in the range from the trot to the pace. As was shown by Hildebrand (1965, 1966, 1967, 1968) and Sukhanov (1963, 1967, 1968, 1974), this feature is defined by a single parameter, which is a quantitative measure of coupling of the fore- and the hindlimb pairs (remembering that the two limbs in a pair act in anti-phase). The common name for this parameter is the "limb phase"; however, Sukhanov himself (1963, 1967, 1968, 1974) termed it the "rhythm of locomotion", and Cartmill *et al*. (2002) named it "diagonality". In the latter research, there is a vivid graphical representation of the useful idea that any symmetrical gait can be simulated by two people walking or running one after another at a fixed distance provided that their step lengths and limb frequencies are equal. If the two move their legs in parallel (limb phase parameter equals zero), they imitate the pace. With opposed stepping (limb phase is 50%), they simulate the trot. Can their combined trackway tell a tracker what did they play – the pace or the trot? Are there any distinctive features between the pace and the trot trackways in simulations or in real animals? The analysis of camelid and equine trackways shows that the distinction is only possible when the trackmaker is known in detail, including its limb length, body length, etc. (Thompson *et al*., 2007; Kienapfel *et al*., 2014). Moreover, the computer trackway simulator (Alexander, 1995) shows that, for a chosen stride length (determinant of the speed), absolutely identical trackways can be produced by the pace and the trot and by any symmetrical gait with an intermediate value of limb phase (from 0 to 100%). Their identity is achieved by adjustment of only a single additional parameter, which

is the length of the body between the fore- and the hindlimbs, known as the "glenoacetabular length". Furthermore, even for a given symmetrical gait, for instance, the exact trot, identical trackways can be produced with a number of different glenoacetabular lengths (first shown by Peabody, 1959). In fact, exactly the same appearance of a trackway can be produced with a wide variety of different combinations of the limb phase and glenoacetabular length values. The aforementioned metaphor of two persons walking one after another helps appreciate this fact vividly. Imagine the third one going along their combined trackway. Let this individual step exactly in the footprints left by the second one. This person can do this being at any distance behind, and should not necessarily move his/her legs in phase with the forerunner. So, the distance from the first person (simulating the glenoacetabular length) and the limb phase relative to the first person can be very different in the first-and-second pair and the first-and-third pair, although the trackway is the same because the footprints of the second and the third person coincide. Generally speaking, in quadrupedal locomotion with symmetrical gaits, the specific trackway geometry is derived from two independent variables, namely the glenoacetabular length and the limb phase (the third variable is the stride length which is associated with speed and can be treated quite separately). Therefore, to solve the symmetrical gait from the trackway of a given stride length (i.e., to find the value of the limb phase), one needs to know the trackmaker's glenoacetabular length, and vice versa. Apparently, the two variables cannot be extracted from the trackway simultaneously. One of them should be obtained from some other source.

In paleoichnology of lower tetrapods, "the problem of two variables" outlined above is entirely dismissed. The trackmaker's glenoacetabular length is traditionally extracted from the trackway by the method of Baird (1952), who measured it as the distance between two points defined therein as follows: "A point on the trackway midline halfway between the two carpi represents the approximate center of the glenoid axis, and a point halfway between the two

tarsi similarly represents the center of the acetabular axis at the same stage in the cycle of locomotion." Thus, the measurement procedure entirely depends on what is this stage in the cycle of locomotion. Baird assumed that, during the locomotor cycle, there was a brief stage when the animal stood with all four feet landed in the four footprints of the trackway at once. More specifically, these four footprints were chosen on the trackway in such a way that the imaginary animal adopted the typical trotting posture with the two limbs of one diagonal in the most protracted position, and those of the other diagonal in the most retracted position. This means that the gait was *a priori* presumed to be the trot (50% limb phase). The additional *a priori* assumption was to choose for the trotting posture those two pedal imprints on the trackway, which are the closest behind the reference pair of manual imprints. With the help of these two assumptions, Baird got an opportunity to reach a single solution for the glenoacetabular length in the trackway puzzle. Sukhanov (1968, 1974) modified the measurement procedure in order to cover faster symmetrical gaits of lizards lacking the stage when all four feet are in contact with the ground at once. He measured the distance along the trackway longitudinal axis from a selected manual imprint to the nearest (posteriorly) footprint of the diagonal hindlimb. Evidently, this gives the same glenoacetabular value as the Baird's method and implies the same limb phase of 50% corresponding to the exact trot. Sukhanov (1968, 1974) concluded that this method gives a good approximation of glenoacetabular lengths measured on lizard bodies directly. This is not surprising for lizards, as far as they really use gaits very close to the exact trot. However, this is questionable for unknown trackmakers of the past. In fact, Baird's method artificially restricts the gait analysis of fossil trackways. For instance, when applied to narrow trackways, it leads to reconstruction of such a great degree of lateral body bending (Smith, 1993), which looks unreal as compared to extant urodelans and reptiles. In fact, the narrow trackways could be readily left by a pacing trackmaker, but Baird's method does not allow for this. In fact, it does not allow for

any considerable shift from the exact trot in the gait reconstruction. Consequently, the restriction is transferred onto the estimation of the second variable involved in determination of the trackway geometry, which is the glenoacetabular length. Notably, in the original description of *Sukhonopus*, Gubin *et al*. (2003) estimated the trackmaker's glenoacetabular length, based on the method of Sukhanov (1968, 1974), implying the trot.

TRACKWAY ANALYSIS

Two trackways were analyzed, the shorter one and the longer one, which will be herein referred to as "trackway S" and "trackway L", respectively. The trackway S (Supplementary material 1) is the specimen PIN 4850/4 stored in the Borissiak Paleontological Institute and exhibited in the Orlov Paleontological Museum. It was described as *Sukhonopus primus* along with the specimen PIN 4850/2 (not analyzed herein), which was chosen as the holotype (Gubin *et al*., 2003). The trackway L (Supplementary material 2) was considered, but not assigned earlier (Rautian, 2002), and the authors of the ichnotaxon *Sukhonopus* (Gubin, Golubev, and Bulanov, personal communication) unequivocally regard it now as *Sukhonopus*. The trackway L crosses the bed of the Strel´na River from the right bank to the left one at the North latitude 60 35.158 and the East longitude 45 31.714 (exposure 9334 of Gubin et al., 2003).

General description of the trackways

The trackway S is almost 2.5 m long, and represents 2.5 strides, i.e., 2.5 cycles of locomotion, including 3 imprints of every limb. The 4th imprint of the left manus is partial and cannot be considered. The trackway L is about 17.3 m long and represents 15.5 strides including 17 imprints of the left pes, 17 imprints of the left manus, 16 imprints of the right pes, and 15 imprints of the right manus (the 13th is missing). No marks of the tail or belly are

present on the trackways. The blurry outlines of the footprints suggest softground conditions at the time of formation. However, judging by considerable footprint depths, the trackmaker's body was unaided by buoyancy. The footprint depths were measured on the trackway S. The pedal and the manual imprints are approximately equally deep and are deeper at the medial side than at the lateral one (see Supplementary material 1). On average, the pedal imprints are 2.4 cm deep laterally and 5 cm deep medially. In the manual imprints, the difference is considerably smaller. On the average, they are 3.4 cm deep laterally and 4.4 cm medially.

The direction of the digits on the left and right imprints of both trackways is bilaterally symmetrical. The absence of declination of the footprint directions to one side of the trackway indicates that it was not a walk in a waterflow like in ichnological experiments on extant newts (Brand & Tang, 1991). For the same reason, it was not a walk across a slope (Loope, 1992). Thus, the producers of both trackways apparently performed truly terrestrial (unaided by buoyancy) walking over horizontal ground. The manual imprints are shaped almost identically on the trackway S and the trackway L (Fig. 1 rows 1, 2). The digit V is short and straight and points forward and a little mediad according to the general turn of the manus. The digits from IV to I are turned inwards more and more with the digit I placed almost at right angles to the digit V. Contrary to the manus, the pedal imprints are shaped somewhat differently on the trackway S and the trackway L (Fig. 1 rows 3, 4). On the trackway S, the digit III points forward, and the imprint of the digit V is not well pronounced except for the last imprint of the right pes (Fig. 1 cell 4A), which is shaped just like the pedal imprints of the trackway L. In the latter, in all the pedal imprints where the digits can be well distinguished, the imprint of the digit V is almost as long as that of the digit IV. In addition, the digit which points forward is the digit IV or even the digit V, not the digit III. This is due to some inward turn of the pes as a whole on the trackway L, while on the trackway S it points forward along the pathway.

Quantitative gait analysis of the trackways

The trackway S was studied by direct measurements on the specimen in the Orlov Paleontological Museum. The trackway L was studied by measurements on the digital photos. When I visited the site of the Strel´na River in summer 2006, the trackway L was covered by approximately 20 cm of water flow. I made step-by-step photos of the whole trackway L with and without the rope grid, which cells were 25x25 cm. Based on this grid, I applied all necessary distortion corrections to each photo and then combined them in a panorama (Fig. 2). Finally, I placed over them the photos without the grid and obtained a clean panorama of the whole trackway L (Supplementary material 2). The following measurements were done on this large photo of as high resolution as 40953x4376 pixels. To check the method robustness, some measurements were also done on the photo reduced to 20% (8191x875 pixels) and purposely saved with low JPEQ quality; its analysis will be referred to as the "rough test" or "analysis C".

For gait analysis, it is necessary to choose equal points on every footprint. Baird (1952) used the footprint center, whereas Padian & Olsen (1984) preferred the midpoint on the posterior border of the footprint instead. In our case, the anterior border of imprints looks more reliable being sharper than the posterior border. Especially sharp are the imprints of digit tips. Also, the footprint outlines are sharper at the bottom and smooth out at the slab surface. Therefore, the tip of the digit III at the footprint bottom have been chosen here as the reference point both for manus and pes (analysis A). In the trackway L, the tip of the digit IV of the hindlimb was employed as an additional reference point (analysis B) because in this trackway this digit is more aligned with the trackway direction than the digit III. In the rough analysis C of the trackway L, the approximate centers of the pedal and manual imprints were used which were purposely located very frivolously. For precise analysis, the footprint

centers are worse than the digit tips because of some blurriness of the heel and wrist outline. On the trackway S, the digit III tips were marked directly on the slab. The procedure with the photo of the trackway L was more cumbersome (Fig. 1 columns B-E) because of more blurry footprints. The sharpest imprints of every limb were selected which are the 9th imprint of the left manus and the 11th imprint of the right manus, the 16th imprint of the left pes and the 12th imprint of the right pes (Fig. 1 column B). Outlines of the bottom area of these imprints were drawn (Fig. 1 column C), and then those of the contralateral limbs were reflected one onto the other and averaged by hand (Fig. 1 column D). These averaged outlines were multiplied and placed over every imprint of the respective limb, so as to match the outline to the imprint boundaries as much as possible (Fig. 1 column E, Supplementary material 2). With the help of these outlines, it was possible to locate the tips of the reference digits (III for manus, III and IV for pes) precisely enough even on the footprints where the traces of these particular digits are much destroyed. For further consideration, it is necessary to note that the length of the pes outline from the heel edge along the digit III up to its tip is 20 cm. Hereinafter, this value will be referred to as the "pes length" of the trackway L. The pes length of the trackway S was obtained by direct measurement of the second left pedal imprint, which is the sharpest one on this trackway (Fig. 1 cell 3A). Its bottom length from the heel edge along the digit III up to its tip is 15.5 cm. Hence, the trackmaker individual of the trackway S was about one quarter smaller in linear dimension than that of the trackway L.

Having located the reference points of every footprint, the distances from each such point were measured to the respective points on the previous and on the next imprints of the same foot, i.e., from pes to pes or from manus to manus imprint on the same side of the trackway. This distance is known as the stride length and corresponds to the distance passed by the trackmaker during a single locomotor cycle. The average stride length of the trackway S is around 83.5 cm (n=8 measurements) and that of the trackway L is 105.4±7.8 cm

(mean±SD, n=60 measurements). In symmetrical locomotion, the step length is exactly equal to half stride length due to the aforementioned anti-phase coordination of the left and right limbs in a pair. Therefore, the steps are approximately 42 cm in the trackway S and approximately 53 cm in the trackway L. The widths of both trackways measured between the digit III tips of the left and right pedal imprints is very close indeed to the respective values of the step lengths being around 47 cm in the trackway S, and 44.0±4.1 cm (n=31 measurements) in the trackway L. The narrowness of the latter, as compared to the former, is partially due to the aforementioned inward turn of the pes, specific to the trackway L. The pedal digit IV is more aligned with the travel direction in this trackway. Using its tips as reference points (analysis B) instead of those of the digit III, gives the trackway L width value of 55.4±4.4 cm. In any case, the close proximity of step lengths to trackway widths manifests that the stride angle, measured from a selected footprint to respective points on the previous and the next footprints of the contralateral limb, is near 90^0 in both trackways. This angle (named "pace angulation" by Baird, 1952) is an indirect representation of the speed of trackmaker progression. For comparison, in the walking trackway of *Varanus komodoensis* with similar values of stride length (89 cm) and pes length (21 cm along digit III), the angulation was no more than 80^0 (Padian & Olsen, 1984). 90^0 angulation of *Sukhonopus* is not as much greater to decide that the trackmaker was running. Either it was walking just a little faster than the Komodo monitor on the trackway considered by Padian & Olsen (1984), or it simply placed the paws a little narrower relative to the stride length than the lizards do.

The next procedure was to locate the midpoints for every pair of the pedal imprints and for every pair of the manual imprints, as Baird (1952) did. In Fig. 3, the pedal pairs are connected by blue segments from the digit III tip of the left imprint to that of the right one (together these segments make a zigzag), and their midpoints are marked by yellow dots. The red segment with the green dot in the middle corresponds to the last manual pair on Fig 3 (see

the complete set of segments and dots in Supplementary material 2). Following Baird (1952), the glenoacetabular length should be measured from this green dot to the second yellow dot counting in backward direction (from the right to the left). This yellow dot is the midpoint of the blue segment which has an opposite inclination to the red segment shown. The opposite inclination is crucial when thinking of the trackmaker as of a trotting animal. The four-limb phase of support is present in the slow trot, which is one of the typical walking gaits of lower tetrapods (Sukhanov, 1968, 1974). It could put all its four feet for a while in the four footprints connected by the red and blue segments, which are oppositely inclined (determinant of trot) and at the same time closest to each other (determinant of short body). There is only one blue segment connecting the pedal pair in *Sukhonopus* representation on Fig. 3, which is even closer to the red segment connecting the last manual pair. However, it is not opposite in orientation to the latter but sub-parallel to it. If some extremely short-bodied trackmaker put its four feet in the respective four footprints (the four right-most ones on Fig. 3) with the left limbs in the most protracted position and the right ones most retracted, its gait would be the slow pace. In fact, this glenoacetabular length is equal to understepping, which is the distance from the reference point of the manus imprint to that of the ipsilateral pes imprint just behind it. If the trackmaker had the glenoacetabular length intermediate between this extremely short value associated with the slow pace and the larger "Baird's value" associated with the slow trot, then its gait would be also somewhere in-between these two opposite symmetrical gaits.

To generalize the analysis, the glenoacetabular lengths were measured for different combinations of the manual and pedal imprint pairs (Supplementary material 2). In Fig. 3, the method is illustrated for the last manual pair represented by the red segment with the green dot on the middle. For visualization, the Hildebrand-Sukhanov chart of symmetrical gaits (Hildebrand, 1966; Sukhanov, 1968, 1974) is placed directly over the trackway under study.

First, the chart is oriented in such a way that its limb-phase axis crossing the chart from pace to trot and to pace again parallels the trackway direction, which is horizontal in Fig. 3. Second, the chart is adjusted to the trackway in such a way that its pace line on the right is aligned with the midpoint between the last two contralateral pedal imprints represented by the right-most yellow dot in Fig. 3; its trot line is aligned with the second yellow dot counting from the right to the left (reverse to the trackmaker's travel direction), and the other pace line on the left of the chart is aligned with the third yellow dot. As a result, the chart period, i.e., the distance from one pace line to the other, is made equal to the stride length of the trackway. Third, the gait chart is multiplied and laid out with the same adjustment to the yellow dots (midpoints between the pedal imprints) along the whole trackway up to its very beginning (on Fig. 3 there is a room for two charts only). In this representation, a segment drawn from the green dot backward to any odd yellow dot corresponds to the glenoacetabular length associated with exact pace, while a segment drawn to any even yellow dot is the glenoacetabular length corresponding to exact trot. Therefore, there is a group of glenoacetabular lengths appropriate for pace, and another group of glenoacetabular lengths appropriate for trot, and the members of these two groups alternate with the interval equal to the step length (half stride and half chart period). The general formula for pacers' glenoacetabular lengths is [(understepping) + N*(stride length)] where N is a non-negative integer. The general formula for trotters' glenoacetabular lengths is [(understepping) + (half stride length) + N*(stride length)]. The intermediate values of the glenoacetabular length imply the lateral-sequence or diagonal-sequence symmetrical gaits depending on the half-period of the chart where this glenoacetabular length falls (Fig. 3).

For complete analysis of the trackway, the described procedure with the Hildebrand-Sukhanov gait chart superposition can be applied starting with the reference point at the midpoint of a segment connecting any pair of the manual imprints. Also, it can be applied

starting with the reference point at the midpoint of a segment connecting any pair of the pedal imprints, but in this case, the glenoacetabular lengths should be measured from posterior to anterior. Notably, the Hildebrand-Sukhanov gait chart should be superimposed with caution: in order to keep the proper position of the lateral-sequence and diagonal-sequence zones of the chart relative to the trackway, the polarity of the limb phase axis should be the same as in Fig. 3 if the reference point is in the middle of the segment connecting the successive pedal imprints from the left to the right, and the polarity should be reversed if the reference point is in the middle of left-to-right manual segments or right-to-left pedal segments. In the latter cases, for visual representation, the gait chart should be turned upside-down as compared to Fig. 3.

For the trackway S, the following mean values were obtained based on direct measurements of the distances between midpoints of the manual and pedal imprint pairs with the reference points at the digit III tips. The approximate resultant formula for all possible glenoacetabular lengths which could ensure the exact pace on the trackway S is ≈[23 + N*83.5] cm where N is a non-negative integer. The respective formula for exact trot is ≈[65 + N*83.5] cm. The accurate glenoacetabular length values for exact pace and exact trot are represented in Table 1. Among the latter, 65.5 cm length corresponding to Baird's method is equal to the estimate of 62-66 cm published by Gubin *et al*. (2003) in the original description of the trackway S (PIN 4850/4). It is not surprising since they used the method of Sukhanov (1968, 1974), which is based on the same method of Baird (1952), differing only technically but not in principle. In trotting lizards, the trackway-based measurement may underestimate the glenoacetabular length because of the lateral bending of the body. Indeed, with the curved spine the midpoints of the shoulder and pelvic girdles come a little closer to each other than in the straight body at rest (Baird, 1952). The maximum possible central angle of the lateral curvature of the body in trotting approaches the value of trackway angulation measured from

a selected footprint to the previous and the next footprints of the contralateral limb. In case of 90^0 angulation, which was aforementioned for *Sukhonopus*, the glenoacetabular length would shorten up to 10% only (this is the chord and arc difference for the angle of 90^0). Actually, the shortening would be even smaller because the step length is produced not only by spine bending, but also by limb protraction and retraction, which are never reduced to zero but usually prevail over spine bending. In addition, the glenoacetabular distance averaged over the locomotor cycle deviates from the straight spine length even smaller because the spine straightens and bends to the other side during the cycle. That is why the fluctuations of the glenoacetabular length can be dismissed for the *Sukhonopus* producer if it was a trotter. If it was a pacer, the lateral bending is irrelevant at all as it does not help increase the stride length in pace. What cannot be dealt with is the possibility of kyphosis like in echidnas (Gambaryan & Kuznetsov, 2013). In this case, the trackway-based glenoacetabular estimate corresponds to its effective functional value but is inevitably smaller than the length of the glenoacetabular segment of the vertebral column measured on the skeleton, and the difference is unknown in principle. However, the lower tetrapods are rarely as much kyphotic.

Statistical analysis of the trackway L

The considerable length of the trackway L allows to analyze it statistically (number n of serial measurements from 26 to 30, see Table 1). Three analyses were performed. The major one (analysis A) relied upon the digit III tips both in the pedal and manual imprints as the basic reference points. The additional one (analysis B) relied upon the digit III tips in the manus but on the digit IV tip in the pes. This is to take into account the peculiarity of the trackway L (as compared to the trackway S) that the digit IV is more parallel to the general trackway direction than the digit III declined somewhat mediad. The last (analysis C) was the

426 rough analysis on the reduced image of the trackway (20% of the original) relying upon the
427 footprint centers. This is to estimate the method robustness. In the analysis A, the
428 approximate resultant formula for all possible glenoacetabular lengths which could ensure the
429 exact pace on the trackway L is ≈[35 + N*105] cm where N is a non-negative integer. The
430 respective formula for exact trot is ≈[88 + N*105] cm. The accurate glenoacetabular length
431 values obtained in the three analyses for exact pace (three solutions corresponding to N = 0,
432 1, 2) and exact trot (two solutions corresponding to N = 0, 1) are represented in Table 1. The
433 larger glenoacetabular lengths (for larger N) were dismissed as obviously unreal.
434 The five solutions were compared with each other by the values of standard deviations
435 (Table 1). The SD value shows the stability of every variant of the glenoacetabular
436 measurement throughout the trackway. From a general point of view, one can reasonably
437 expect that in the series of measurements illustrated by Fig. 3, the SD of any longer
438 measurement should be greater than that of any shorter one. Indeed, the further posterior are
439 the pedal imprints from the manual ones, the more independent should be their steps. Far
440 away, the animal could walk in a different way. Accordingly, SD of a glenoacetabular
441 measurement is expected to increase monotonously with the increase of this measurement
442 mean value. However, the plot of SD vs. mean of the possible glenoacetabular lengths for the
443 trackway L gives an unexpected minimum at the "middle pacer" solution (Fig. 4). Not only
444 the "long trotter" and "long pacer" show greater SD (expected), but the "short trotter" and
445 "short pacer" show the same (unexpected). This peculiar pattern is the repeated in all three
446 analyses, and all the three plots are very well approximated by binomial curves (see the
447 formula with R^2 value for analysis A on Fig. 4). The only important difference between the
448 three analyses is that in the analysis A, based on the digit III tip of the pedal imprints, SD
449 values are a little smaller for every glenoacetabular solution. Thus, analysis A can be
450 regarded as a little more reliable than the other two which SD values almost coincide with

each other. The glenoacetabular means of the rough analysis C based on the footprint centers are almost the same as those given by the analysis A, while the means produced by the analysis B are a little smaller. Obviously, this is because the tip of the digit IV on which this analysis is based protrudes on the pedal footprints of the trackway L a little forward relative to the digit III tip on which the analysis A is based. Overall, digit III tip proves to be the best reference point for the pedal imprints.

The unexpected appearance of the definite and robust (supported by the rough analysis C) "middle pacer" minimum on the SD vs. mean glenoacetabular length plot (Fig. 4), instead of the monotonous proportional growth of the two, has an efficient explanation. The SD minimum is pointing on the manual and pedal imprints which were produced least independently from each other. The fact that the "middle pacer" distance was kept most constant throughout 15.5 locomotion cycles may indicate that it is based on a firm structural background. The only thing which can ensure the mutual dependence between the fore and hind limb pairs is their connection by the trunk. Therefore, the minimum SD is pointing on the true glenoacetabular measurement. For the "middle pacer", it is 140.2±3.5 cm based on the analysis A (Table 1). Binomial approximation shows that the true glenoacetabular length of the trackmaker could be a little shifted from the "exact middle pacer" toward the "short trotter". Solving the minimum of binomial approximation for SD in the analysis A, whose formula is written in Fig. 4, gives the glenoacetabular length of 119.0 cm (red arrow on Fig. 4). Therefore, the true glenoacetabular length was most probably somewhere in-between 140 cm and 119. Respectively, the gait was shifted from the exact slow pace to the slow pace-like walk in the lateral sequence, i.e., just a little to the right from the line of exact pace on the Hildebrand-Sukhanov chart.

Comparison of the trackways with skeletal proportions of *Deltavjatia*

To obtain dimensionless values of the stride lengths and the glenoacetabular lengths, they were divided by the length of the pedal imprints from the heel edge to the digit III tip, which is 15.5 cm in the trackway S and 20 cm in the trackway L. The stride length of the trackway S normalized in this way is on the average equal to 5.38 p.l. (pes lengths). The normalized stride length of the trackway L obtained with the most reliable analysis A (based on the pedal digit III) is 5.27±0.39 p.l. The approximate formula for all possible normalized glenoacetabular lengths which could ensure the exact pace on the trackway S is ≈[1.5 + N*5.4] p.l., and on the trackway L is ≈[1.8 + N*5.3] p.l. where N is a non-negative integer. The respective formulae for exact trot is ≈[4.2 + N*5.4] p.l. for the trackway S, and ≈[4.4 + N*5.3] p.l. for the trackway L. The accurate normalized glenoacetabular length values are represented in Table 1. The most probable normalized glenoacetabular length given by the minimum SD in the analysis A of the trackway L (Fig. 4) is between 7.01±0.18 p.l. and 5.95 p.l. The upper limit corresponds to the "middle pacer" (represented by the very close value of 6.89 p.l. on the trackway S); the lower limit is the solution for the minimum point on the binomial approximation for SD plot in Fig. 4 normalized by the pes length. Roughly, the glenoacetabular distance of the *Sukhonopus* producer was most probably between 6 and 7 p.l. This range can be checked against glenoacetabular-to-pes length ratios in pareiasaurian skeletons.

The glenoacetabular-to-pes length ratio (normalized glenoacetabular length) can be estimated on the available skeletal material of pareiasaurians. The mounted skeletons of *Scutosaurus karpinskii* (which is larger than the *Sukhonopus* producer) exhibited in the Orlov Paleontological Museum of the Borissiak Paleontological Institute are not naturally articulated and considerably incomplete. Critically for the method, there is no specimen that combines the complete pes and the complete vertebral column together. On the other hand, there are four skeletons of *Deltavjatia rossica* (which is smaller than the *Sukhonopus*

501 producer) exhibited in the Vyatka Palaeontological Museum (the specimens KPM 232, 234,
502 289, 290), which are almost complete and naturally articulated as the animals died stuck in
503 clayey silt. Their glenoacetabular and pes length measurements as well as the ratios thereof
504 are represented in Table 2. All the glenoacetabular lengths of *Deltavjatia* skeletons are
505 considerably greater than the 62-66 cm estimate for the trackway S by Gubin *et al*. (2003),
506 while the pes lengths are, on the contrary, considerably smaller than 15.5 cm length of the
507 best pes imprint on the same trackway. The glenoacetabular-to-pes length ratios from Table 2
508 are plotted as yellow arrowheads in Fig. 3 against the glenoacetabular scale superimposed
509 onto the trackway L map and against the respective limb-phase axis of the Hildebrand-
510 Sukhanov gait chart. The normalized glenoacetabular lengths of the specimens KPM 289,
511 290, and 234 are 5.88, 6.12, and to 7.15 p.l., respectively (Table 2). This variety is very close
512 indeed to the range from 5.95 to 7.01±0.18 p.l. suggested by the trackway L. Only the
513 specimen KPM 232 with the normalized glenoacetabular length of 8.10 p.l. falls much above
514 this range. Respectively, on the Hildebrand-Sukhanov gait chart it falls in the area of the
515 diagonal-sequence symmetrical gaits (black area on Fig. 3) known among tetrapods only in a
516 restricted number of mammals mainly of arboreal lifestyle (Hildebrand, 1967). This extreme
517 deviation of the specimen KPM 232 may probably result from a longitudinal compression of
518 the digits in the course of deposition (Fig. 5). However, the mean normalized glenoacetabular
519 length for all four *Deltavjatia* specimens, including the deviating KPM 232, is 6.81 p.l. that is
520 well inside the trackway-suggested range.

521 Furthermore, the three skeletal ratios that fit the trackway-suggested range (KPM 234,
522 289, 290) are unequally reliable. Measurement of the glenoacetabular distance was a little
523 problematic. Normally, it should be measured along the curve of the vertebral column from
524 the level of glenoids on the shoulder girdle to the level of acetabula on the pelvic girdle.
525 However, in the specimen KPM 234 the latter is destroyed, therefore, the level of acetabula

was located by the femoral heads. In the specimen KPM 290, the shoulder girdle is destroyed, and the glenoacetabular length was measured from the occiput. The specimen KPM 289 is distinguished by the best 3D preservation (Fig. 6). In its left pes (Fig. 5.1), the ends of the digits IV and V are lost, but the digit III is complete and not compressed longitudinally, and the space for the distal tarsals is kept natural. Therefore, the pes length could be perfectly measured from the tip of the digit III to the distal border of the astragalus located just proximal to the intratarsal joint (arrows on Fig. 5). As was aforementioned, this specimen has the lowest glenoacetabular-to-pes ratio of the four skeletons studied. Its value of 5.88 p.l. is located just at the lower end of the range suggested by the trackway L (compare positions of the right-most yellow arrowheads on Fig. 3 and the red arrow on Fig. 4). This is most far apart from the exact pace but is still closer to it than to the exact trot. The corresponding gait is the slow pace-like walk in the lateral sequence.

REVERSE ENGINEERING

The conclusion of the above analysis definitely goes beyond the locomotor constraints known for extant animals, because today the lower tetrapods never use the pace-like gaits due to their static instability in the case of the sprawling limb posture (Sukhanov, 1968, 1974). However, the dynamic stability of pace can be achieved with body rocking from side to side as in a man who attempts to walk on widely abducted legs. This principle was implemented in a traditional Russian kinetic toy called a "walking-rocking bull-calf" that passively goes down a shallow-inclined plank (Supplementary material 3) or over a horizontal table, being pulled by weight on a thread kinking over the table edge. The toy frequently falls over when going from the inclined plank onto the horizontal surface. However, being driven with the thread, the toy always gently stops at the table edge, because there the thread becomes vertical and ceases pulling the toy forward. The toy is simply built, each leg being a rigid

pendulum attached to the main body by a simple (i.e., possessing one degree of freedom) hinge, which has an axis of rotation perpendicular to the sagittal plane, and the amplitude is limited by stoppers preventing falling forward or backward when the toy stands still. The end of the leg is not a point, but a sole area that can be wide or rather narrow, flat or gently concave (like in a rocking chair). The pendular leg oscillations coincide with body rocking from side to side (also termed rolling), and the resultant gait of the toy is the exact pace with the duty factor a little above 50%. The quantity above 50% corresponds to the time interval when all four feet contact the ground simultaneously. The presence of this quadrupedal phase of support distinguishes the bull-calf's gait as the slow variant of exact pace.

The same mechanical principle is currently developed in robotics, being referred to as quadrupedal passive-dynamic walking (Smith & Berkemeier, 1997; Remy *et al*., 2010a, 2010b). The passive-dynamic robot makes use of its own natural pendular dynamics properties to propel itself down a shallow incline without needing any motors, sensing or control. In fact, it is a passive mechanism that pumps the potential energy of gravity against hinge friction and other items of energy dissipation, and thus sustains the periodic limb motion remaining dynamically stable against small disturbances.

Based on the principle of the passive-dynamic walking-rocking bull-calf and on the dimensions of *Sukhonopus*, the natural-sized pacing model of a pareiasaur (Fig. 7) was built. The naturalistic skin envelope was made of acrylic plaster with a light iron frame mounted inside for legs' suspension. The suspension included the transverse hinge axis made of 23 mm thick polished iron rod, on the body side, and the sleeve made of bronze, on the leg side. The diameter of the foot sole, both in the hind- and in the forelimbs, was 19 cm, just a little less than the 20 cm long pedal imprints on the trackway L. The glenoacetabular length was 112 cm from the glenoid hinge axis of the forelimbs to the acetabular hinge axis of the hindlimbs. The 112-to-19 cm ratio is 5.9, which corresponds to the glenoacetabular-to-pes ratio of the

Deltavjatia specimen KPM 289 (Table 2). With the same 112 cm glenoacetabular length, the pes could be made as short as 16 cm (roughly equal to 15.5 cm long pedal imprints on the trackway S), and then their ratio would be equal to 7 which corresponds to exact middle pace on the trackways (Table 1). Thus, 112 cm is a kind of a compromise glenoacetabular value for the complete set of measurements on the trackways and skeletons. The total body length of the model from the nose to tail tip was 185 cm, according to its ratio ≈5/3 to the glenoacetabular length observed in pareiasaurians, which have been measured. The weight of a living pareiasaur of this length could be probably up to 300 kg (just a little heavier than a big wild boar or pygmy hippopotamus *Choeropsis*). The weight of the walking-rocking pareiasaur model due to its hollowness was about 90 kg including ≈2 kg of lead shot additionally loaded in each heel to enhance the limb ability to swing forward while walking on horizontal ground. The transverse distance between the midpoints of the left and right feet was close to 45 cm, like between the pedal digit III tips on the trackways studied. Each foot surface was gently skewed in a transverse direction, making the distance from the hinge axis a few centimeters greater medially than laterally in order to smooth out body rocking from side to side. The limb length measured from the hinge axis to the foot sole surface was 55-60 cm. The anterior and posterior stoppers, protected with teflon, limited the amplitude of the pendular oscillations of the limb to $\approx 45^0$ which, combined with the limb length, gives the maximum possible step length of about 45 cm, just a little more than observed on the trackway S. However, in the natural passive-dynamic pacing of the model, its limbs did not swing from stopper to stopper, but employed the approximately twice narrower swinging angle. Therefore, the step length observed in the model was about 20 cm (a little more than the pes length), and its stride composed of two steps was about 40 cm, while on the trackway S it is roughly 80 cm and on the trackway L 105 cm. At the beginning of usage, the hinge friction hindered proper coupling of oscillations of different legs, and hence, the steps were

sometimes even shorter than 20 cm (see Supplementary material 4, which was recorded at the very creation of the model), but soon the sliding surfaces became reseated to each other and the regular pace was achieved.

The model was used in the lesson on paleontology for children at the Biological Laboratory of the Polytechnic Museum, Moscow, Russia. The lesson began by digging pareiasaurian bones from the sand basin. The bones were copied from one of the small specimens of *Scutosaurus* exposed in the Orlov Paleontological Museum of the Borissiak Paleontological Institute. Then, the children mounted the bones into an articulated skeleton on the special frame and studied its proportions, in particular, the pes and glenoacetabular lengths. After that, the cast of the trackway S (Supplementary material 1) was presented to the children, and the problem of the gait-and-trackway interconnection via pes-to-glenoacetabular ratio was introduced with the help of sticks of appropriate proportions superimposed on the trackway cast (similar to the red, blue, and magenta lines on Fig. 3). Having realized that the pace is the only possible gait to solve the problem, the children approached the idea of rocking walk themselves. Finally, the model appeared on the scene, and children got an opportunity to walk with it.

The model walked on the horizontal floor driven by children instead of walking on an inclined plane (Fig. 7; Supplementary material 4). Three 10-12-years old children could do it easily: one pulling the model forward by a rope, and the other two helping it rock from the left and right sides. After some training, rocking could be assisted by one sole person. The model was used regularly from the beginning of 2014 up to the end of 2016 and probably traveled a total of ten or even a few tens kilometers, but only once required bolt tightening and other minor tunings. Finally, the attachment of the hinge axis for the left hindlimb broke at its base because of the initial welding defect. If the welding here was as robust as in the other limbs, the model could probably safely walk until now, because no other malformations

were discovered at its breakage. However, the reason for the crash is not only the welding defect, but the inherent collisional nature of this walking technique. Rocking from side to side, especially with the sprawling limb posture, is inevitably associated with hard limbs' striking against the ground when the body falls from the left limbs onto the right ones or vice versa. The major fault of the lessons with the walking pareiasaur model was the feet clattering (Supplementary material 4). Obviously, the hindlimb is subject to harder collisions, because the limbs stomp against the ground at the moment, when they are swung anteriorly, the forelimb under the head and the hindlimb under the common center of mass of the body.

DEVELOPING AND TESTING PREDICTIONS

Could real pareiasaurs travel by means of the rocking pace, like the *Sukhonopus* producer model, but unaided by children and making at least twice longer steps and strides actually found on the trackways? There is some important evidence that they could. First of all, it is the inward-turned manus which is the distinctive feature of all *Sukhonopus* specimens as well as of the articulated *Deltavjatia* skeletons (Figs. 6, 8). The inward-pointing claws of the forelimbs can be regarded as an important adaptation for rocking locomotion because this feature enhances the ability to push the body against the ground to the contralateral side (Kuznetsov, 2011). In fact, the inward-turned manus plays the same role in pumping the rocking motion as the people pushing the *Sukhonopus* producer model from side to side. It can be hypothesized that the rocking pace was employed by other extinct trackmakers, whose trackways show symmetrical gait and the inward-turned manus, *e.g.*, in *Limnopus* (Baird, 1952; Martino, 1991).

The forward direction of the pedal imprints manifests that the main activity of the hindlimbs was propulsion, the same as the role of the children pulling the *Sukhonopus* producer model forward by the rope. However, there are the aforementioned inward turn of

651 the pedal imprints on the trackway L, and deepening of the pedal imprints to the medial side
652 on the trackway S. These features indicate that the hindlimbs could aid the forelimbs in
653 pumping the rocking motions. Although the inward turn of the pedal imprints on the
654 trackway L is not as sharp as in the manual imprints (Fig. 3; Supplementary material 2), it is
655 still striking because of the fact that the inward-turned hindlimb is extremely rare among
656 quadrupedal tetrapods. Among extant species, the rare exception is represented by the tracks
657 of wombats (Triggs, 2003). The pedal imprints of the trackway S have the digit III pointing
658 forward without any inward turn, but are deepening, on the average, from 2.4 cm at the lateral
659 side to 5 cm at the medial one with the difference of 2.6 cm (Supplementary material 1). The
660 manual imprints are also deepening latero-medially but smaller, on the average, from 3.4 to
661 4.4 cm with the difference of 1 cm only. In the hardware model, both the fore- and the
662 hindlimbs were made with the equal latero-medial skew of the sole of about 5 cm. On the
663 hard floor, such feet do not produce inclined imprints but serve to soften transition from the
664 limbs of one side to those of the other when rocking.

665 In the walking model of the *Sukhonopus* producer, all the muscular activity is shifted
666 onto the children who pull it forward for propulsion and push from the sides for rocking.
667 Therefore, only passive functions are left for the limbs of the model, which support it against
668 the force of gravity and swing freely forward for the next step. However, even in this passive
669 performance, the fore- and the hindlimbs are somewhat different. It can be supposed that the
670 collision at touch-down moment is somewhat greater in the hindlimb, because the limbs hit
671 the ground in a protracted position. When protracted, the hindlimb is closer to the center of
672 mass of the body and takes upon more of its weight than the forelimb being landed
673 somewhere under the chin. The harder collision at touch-down moment may be one of the
674 reasons why the hindlimb hinge was the first to break in the model. Further, by the end of the
675 contact phase, when the two ipsilateral limbs are going to leave the ground, they have

reached a retracted position and, in this moment, the forelimb is closer to the center of mass of the body. Therefore, it can be supposed that the forelimb plays a greater role in the final push towards the contralateral side. This push is an active effort playing the same role in pumping the energy in the rocking motion as the children drivers at the sides of the model. The main actuators for this push were probably the abductor muscles of the shoulder and hip joints, such as the *musculus dorsalis scapulae* in the forelimb (Fig. 9) and the *musculus iliofemoralis* in the hindlimb. They employ the secondary degree of freedom in this joint, which is the rotation of the humerus and the femur about the horizontal axis passing in cranio-caudal direction. Having been activated by the end of the limb contact phase, the abductor muscles push the body to the other side and then, after the limbs lose contact with the ground, the continuing contraction of the abductor muscles causes further elevation of the limbs and thus increases the clearance of the feet in the swing phase.

In the hardware model, this degree of freedom was absent. As to the muscular replacement for the children pulling the model forward by the rope, most efficient in this respect are the hindlimb retractors, and the best time to activate them is the end of the contact phase when the hindlimb is most retracted and, hence, its contact with the ground is shifted most posteriorly relative to the animal trunk. In this position, the line of action of the ground reaction force, which connects the pes and the common center of mass of the body, is most inclined forward, and thus the hindlimb retractor muscles develop the greatest propulsive thrust. Summing up the above consideration, by the end of the contact phase of the left or the right limb couples, the *Sukhonopus* producer had to "switch on" the propulsive action of the hindlimb retractors and the transverse pushing action of the forelimb abductors, in order to compensate for energy dissipation during the stride mainly associated with collision of the limbs with the ground at touch-down as well as with minor forces of friction and drag.

However, in the model the difference between the fore- and the hindlimbs is not as considerable as was supposed in some earlier studies. Rautian (2002) claimed that *Sukhonopus* (not yet named at the time of that publication) shows limited ability of the forelimbs to perform walking movements as compared to the hindlimbs. This claim contradicts the actual trackway features. Indeed, the left and the right manual and pedal imprints are located at the same widths. Also, they have nearly the same depths according both to the literature on *Pachypes* (Valentini *et al*., 2008) and to the measurements of the trackway S of *Sukhonopus*. The pedal imprints are deeper than the manual ones medially (the average values for pes and manus are 5 vs. 4.4 cm) but shallower laterally (2.4 vs. 3.4 cm). Valentini *et al*. (2008), based on the trackway *Pachypes*, claimed that pareiasaurian forelimbs were semiplantigrade and sprawling, and the hindlimbs were digitigrade and erect. They termed this "the dual-gait" which is misleading because the limb posture is the spatial property, while the gait is a temporal property by definition (Sukhanov, 1968, 1974). The supposed posture difference was derived by Valentini *et al*. (2008) from the presence of sliding traces in the pedal imprints and their absence in the manual ones of *Pachypes*. From this fact, Valentini et al. concluded that the trackmaker's hindlimbs produced the forward thrust (propulsion), and the forelimbs did not but "had primarily the role of sustaining the heavy anterior trunk". The foregoing analysis agrees with this conclusion, but with an addition that the forelimbs had also the active role of pushing the body from side to side, and the hindlimbs had also the role of sustaining the heavy posterior trunk. However, the following conclusion of Valentini *et al*. (2008) that the non-propulsive role of the forelimbs vs. propulsive role of the hindlimbs implies their different posture, semiplantigrade sprawling of the former vs. digitigrade erect of the latter, cannot be accepted. First, transition to digitigrade and erect posture is not a necessary prerequisite to perform propulsion. Second, there are no direct traces of the supposed posture differences in *Sukhonopus* and *Pachypes*

(which could be the same ichnogenus according to Valentini *et al*., 2009). Indeed, the pedal imprints are not located narrower than the manual ones, which should be the case if only the hindlimbs were erect. Also, the manual imprints are shorter in fact than the pedal ones, while the opposite should be found if only the hindlimbs became digitigrade. Rather, the shortness of the manual imprints implies that the forelimbs' posture was semiplantigrade (in accordance with Valentini *et al*., 2008) but the hindlimbs were entirely plantigrade.

A possible important evidence for the validity of the pareiasaurian walking technique proposed here is supplied by the available data on the limb bone histology of pareiasaurs (Canoville & Chinsamy, 2017; Boitsova *et al*., 2019). One of the major purposes of the investigations cited was to solve the old-standing terrestrial-vs.-semiaquatic dilemma of the pareiasaurian lifestyle. Typically, the long bones of terrestrial tetrapods have a classic tubular structure with the external tube of compact bone, the central marrow cavity, and rather thin transitional spongy layer between the two, composed of the variously oriented tiny trabeculae with small lacunae between them. Contrary to that, some semiaquatic tetrapods have a thickened external tube of compact bone with respectively constricted central marrow cavity. For instance, the latter is represented by a thin canal in the ribs of the sea cow *Hydrodamalis* (personal observation). This replacement of a low-density marrow by heavy bone compacta is regarded as a means to decrease the total body buoyancy and allow the body of the tetrapod to be effortlessly submerged in spite of the presence of the air in the lungs. The classic tubular bones could be expected for pareiasaurs, based on the recent isotopic analysis that supports their terrestriality (Canoville *et al*., 2014). However, the bone histology shows a much unexpected structure (Canoville & Chinsamy, 2017; Boitsova *et al*., 2019). Both the peripheral compacta and the marrow cavity were replaced by spongiosa in the long bones of the pareiasaurian limbs (and to a less extent in the other bones). On the surface, it is observed a diminishing compact layer that immediately came into the spongiosa, gradually becoming

more and more cavitated towards the bone center with trabeculae entering even the very core where the free space for the marrow is normally found in the long bones of terrestrial tetrapods.

Although unexpected, this bone histology can be readily understandable from a biomechanical standpoint. The tube is more preferable than a solid rod of the same material, with same length and same mass (this implies the same cross-sectional area of the tube walls and the rod) if its task is withstanding the bending loads. In this situation, one side of the structure is compressed, the other is extended, while the middle part is neither compressed nor extended, and hence, does not participate in the load bearing. The farther is the point from the middle part, the greater it is loaded, and the greater is its role in resisting the deformation. That is why the hollow tube is better than the rod of the same mass – the material is redistributed from the less stressed central area to the periphery. Normally, the bending loading of the long limb bones prevails (Alexander, 1989), and that is why they are tubular. However, if the bones were loaded by strictly longitudinal forces, there would be no difference between the tube and the solid rod structures, in the first crude approximation, because the longitudinal load is evenly distributed over the cross-sectional area irrespective of its configuration. Indeed, as soon as the passive-dynamic walker cannot switch on actuator at the limb hinge (muscles of glenoid or acetabulum) immediately when the limb hits the ground, the limb acts as a strut, not as a lever *sensu* Gray (1944). In other words, the ground reaction force at the touch-down moment passes strictly along the general limb axis – from the contact point of the foot towards the point of suspension to the body at the proximal hinge (see the blue ground reaction force vector acting on right limb on Fig. 9). That is why the rocking walker does not necessarily need tubular bones in the limbs.

To answer why the spongy bones are better for the rocking walker's limbs than the compact bones, either tubular or solid, of the same length and mass, a second approximation

775 is required. Under the same longitudinal loading, the spongy bone undergoes greater
776 longitudinal deformation, because its tiny trabeculae and the walls of its tiny bubbles have
777 free spaces around to decline compliantly from the line of the longitudinal external force. In
778 fact, the tiny trabeculae and laminae are locally bent in various directions. The greater
779 compliance is advantageous to withstand hard collisions, as in the head-hitting goats and
780 pachycephalosaur dinosaurs (Alexander, 1989). Notice the heavy clattering of the
781 *Sukhonopus* producer model produced when the next feet meet the ground (Supplementary
782 material 4). It is known that the major energetic expenses in passive-dynamic walking are
783 associated with kinetic energy dissipation at collisions when feet strike the ground (Ruina *et*
784 *al*., 2005). Therefore, it can be concluded that the spongy structure could have been better for
785 pareiasaurians because it saved their limb bones from compression fractures at high-energy
786 impacts. Furthermore, the intense internal remodeling of their bones (Canoville & Chinsamy,
787 2017; Boitsova *et al*., 2019) may indicate that the microscopic fractures did frequently occur
788 but were persistently repaired. It is herein hypothesized that the lifetime microscopic
789 compression fractures will be found in future studies of pareiasaurian bone histology.
790 Noteworthy, the surface compact layer is greater reduced on the ventral (inner) side of
791 pareiasaurian long bones of the limbs than on their dorsal (outer) side. To explain this, notice
792 the limb action at the touch-down collision in the transverse plane (see the right limb with the
793 blue vector on Fig. 9). In this view, the sprawling limbs are bow-shaped, because the elbow
794 and the knee are bent outwards, and hence, displaced aside of the general longitudinal axis of
795 the limb, which connects the foot with the glenoid or acetabulum. With a rocking pace, when
796 the foot strikes the ground, the collisional ground reaction force (blue vector on Fig. 9) most
797 probably acts on the sole along the general longitudinal limb axis pointing to the glenoid or
798 acetabulum but passing medial to the bowing skeleton. So, this force tends to bend the limb
799 in the ventral direction even further, causing tension on the outer side and compression on the

inner side of the bones. As was aforementioned, the external layer of compacta is useful in the presence of bending loads. However, if loading is collisional, there is a risk to break the bone, and the compliant spongiosa is necessary on one side of the bone in order to dampen collision and dissipate the kinetic energy of the body falling from one limb onto the other. Finally, there is a question, on which side of the bowing limb, convex or concave, it is safer to place the compliant spongiosa, and on which side the non-compliant compacta should be expected? Physically, the same problem was met by the old-time plumbers who were used to bend iron waterpipes after making them red-hot at the desired bending point with a blowtorch. The wall of the waterpipe can be neither considerably extended on the convex side, nor considerably compressed on the concave side. However, it can be either torn on the convex side, which makes a leaking hole, or folded on the concave side, which is not harmful. Therefore, the plumbers red-heated the waterpipe at the concave wall of the future bend to help it fold easier. Just for the same reason, it is better for bone bending compliance to place the deformable spongiosa primarily on the concave side of the bowed limb. Clearly, the elasticity of ligaments on the lateral (outer) side of the elbow and the knee joints (cyan stripes on Fig. 9) greatly enhanced the overall capacity of the limb as a shock absorber.

In short, it can be concluded that the passive-dynamic rocking-pacing technique of locomotion, which is hypothesized for pareiasaurs on the basis of trackway and postcranial analysis, requires rigid strut-like limbs but compliant bones. This seemingly paradoxical requirement has found, however, a possible line of evidence in the peculiar bone histology of pareiasaurians that seemed puzzling by itself, too. Therefore, a reciprocal reinforcement of a number of hypotheses is immediately obtained, namely, that *Sukhonopus* was produced by a pareiasaur, that pareiasaurs were terrestrial, that their gait was the rocking pace in spite of the sprawling limb posture, and that their unusually spongy limb bones served for terrestrial locomotion as shock absorbers. Some other large continental Permian tetrapods, namely

caseids (Synapsida: Caseasauria), shared with pareiasaurs the specific spongy bone tissue in the limb segments (Canoville, Chinsamy, 2017; Boitsova et al., 2019). Probably, this peculiar and yet unexplained feature is indicative of a similar locomotion technique, that is the rocking pace, as the inward-turned manual imprints can manifest this locomotion technique on the trackways.

Among the extant tetrapods, only echidnas use a similar locomotion technique (Gambaryan & Kuznetsov, 2013). These archaic mammals are also characterized by the sprawling limb posture, which contrasts with parasagittalism of therians (marsupials and placentals). Also, they share with pareiasaurians the inward-turned manus which appears to be crucial for pumping rocking motion and which is rarely found in therians. However, despite the sprawling limb posture, echidnas produce a narrow trackway, quite different in this respect from pareiasaurians and more similar to parasagittal mammals, i.e., therians. This narrowness is associated with a very large value of pace angulation in the published long-beaked echidna (*Zaglossus*) trackway (Gambaryan & Kuznetsov, 2013). Measured from a selected pedal pad imprint (it is a small and thus reliable reference point) to the preceding and the following imprints of the contralateral pedal pad, the echidna's angulation can be found to be just a little less than 140^0 against approximately 90^0 in *Sukhonopus*. Notably, the angulation value of 130-150^0 exactly corresponding to echidna, was reported for the late Permian trackway from South Africa ascribed to dinocephalians (Smith, 1993). The author based his trackmaker reconstruction on the method of Baird (1952), and thus was forced to draw it on the trackway in the trotting position. He even came to the conclusion that the narrowness of the trackway resulted from extreme lateral bending of the body. This conclusion was later supported by Hopson (2015). It is based on the seemingly reasonable assumption that the central angle of body curvature in lateral bending is directly proportional to the footprint angulation on the trackway. However, all this inference is true only in the

framework of trotting hypothesis. Echidna's gait is very far from trot (Fig. 3), and their trackway narrowness together with the great pace angulation is based on quite different kinematic features than the lateral bending of the body which they do not use at all (Gambaryan & Kuznetsov, 2013). Based on 140^0 angulation, as well as on the inward turn of the manual imprints on the trackway described by Smith (1993), it can be reasonably hypothesized that the locomotion of the trackmaker was close to that of echidnas. In one respect, it looks more similar to *Sukhonopus*. In both trackways, there is no overstepping found in the long-beaked echidna. Overstepping means that the pes is landed not behind but in front of the imprint of the manus produced just before. This is due to the greater swinging range of the limbs.

The gait of echidnas is not the exact pace (Fig. 3). Their ipsilateral fore- and hindlimb motions are somewhat decoupled, which results in a four-beat walk close to pace but not the pace itself. "Four-beat" means that the two ipsilateral limbs touch the ground a little out of phase and so the beats of all the four limbs can be heard. Theoretical consideration of two-dimensional passive-dynamic quadrupedal walking (Smith & Berkemeier, 1997) indicates that the four-beat gaits are not as resistant to disturbances, as are the two-beat gaits (in the 2D modeling there is no difference between the pace and the trot). This means that even a small disturbance can destroy the regular limb cycling, and hence, the same gait cannot be sustained from stride to stride. According to the 2D modeling, the stable four-beat passive-dynamic walking can be theoretically achieved through placing inside the trunk of additional mass, which can wobble in antero-posterior direction relative to the rest of the trunk (Remy *et al*., 2010a). In the 3D reality, echidnas employ for this purpose the axial rotation in the vertebral column, which allows rolling the fore and hind halves of the body relative to each other (Gambaryan & Kuznetsov, 2013). This was successfully modeled in 2004 for demonstration of echidna's mechanism in the lectures of the author. The bull-calf toy was cut

875 by halves, cranial and caudal, which then were connected again by means of a hinge on the
876 back with the longitudinal axis of rotation (the white line on Fig. 10). This modified toy
877 began performing a stable echidna-like four-beat walk (Supplementary material 5), which is
878 40 percent faster than the initial exact pace (Supplementary material 6). The collisions
879 became softer, in accordance with the theoretical considerations. The speed increment is due
880 to the appearance of body yawing which increases the stride length (cf. Supplementary
881 material 5 and 6), while the frequency of limb motions remains the same based on the passive
882 pendular dynamics. It is quite plausible that pareiasaurians could enhance their passive-
883 dynamic walking in the same way, that is by employing the axial rotation of the spine. This
884 possibility is shown by a rather unusual horizontal orientation of the articular facets of
885 zygapophyses of their presacral vertebrae (Fig. 11). In the majority of extant and extinct
886 tetrapod groups, the facets of all vertebrae are oriented radially (i.e., along the radii to the
887 vertebral centrum as seen from anterior or posterior side). Exceptional are the pre-
888 diaphragmatic thoracic vertebrae of mammals, which orientation is tangential (also called
889 horizontal). In mammals, this tangential facet orientation is known to enhance the axial
890 rotation in the intervertebral joints (Rockwell *et al*., 1938; Gregersen & Lucas, 1967; Jones *et*
891 *al*., 2020), and it could probably have the same effect in pareiasaurians. This is just what is
892 needed for decoupling of the ipsilateral fore and hind limbs in a passive-dynamic walk. The
893 barrel-shaped rib cage of echidnas looks quite similar to those of many Paleozoic reptiles,
894 *e.g.*, pareiasaurs themselves and also Diadectomorpha, Caseasauria, Dicynodontia. The same
895 feature is also known in ancient amphibians, such as *Eryops* and even *Ichthyostega*, although
896 their rib cage is not yet closed on the sternum. The barrel-shaped rib cage is obviously
897 irrelevant for extensive lateral bending of the spine employed in trot-like locomotion of the
898 lizard type. However, echidnas show that it is quite relevant for axial rotation of the spine
899 employed in the pace-like walk. The *Deltavjatia* specimen KPM 289 shows the spine bent to

900 the left in the death agony (Fig. 6). However, if its gait was actually as close to pace as the
901 preceding analyses have shown, the ability for lateral bending could hardly have any use in
902 forward progression.

903 Even if pareiasaurs used the axial rotation of the spine to decouple the ipsilateral fore-
904 and hindlimb motions like echidnas do, there are two reasons to assume that the walking
905 collisions in echidnas are much smaller. It is not only due to much smaller body mass, but
906 also due to the narrow trackway. Therefore, the spongy limb bones are unnecessary to
907 echidnas. However, the short-beaked echidna *Tachyglossus* was reported to possess a very
908 peculiar and yet unexplained feature which can serve as a shock absorber. It is the hollow
909 femoral head, bearing inside the cartilaginous sphere, a rather voluminous cavity filled with
910 collagen (Thorp & Dixon, 1991). The collagen is more compliant than the cartilage and
911 allows the femoral head deform more at the foot strike with the ground. On the other hand,
912 the hollow cartilaginous femoral head may be a juvenile feature. Personal observations on
913 macroscopic dissections of the femora of two adult individuals of long-beaked echidna
914 (*Zaglossus*) did not confirm the existence of such a peculiarity in this genus. The femoral
915 head is entirely composed of spongy bone with a thin cartilaginous coating. Only in one of
916 the two individuals, there was a small cavity inside the spongy mass.

917 In general, the rocking walking technique of echidnas looks like the last remnant of
918 some ancient type of terrestrial locomotion, which was possibly more widespread or even
919 common in the Permian, when pareiasaurs, and many other barrel-bodied large tetrapods
920 lived. If so, one may ask, why the rocking pace was "popular" then but not now. Initially, it
921 was hypothesized that the side-to-side rocking motion was useful when walking over swamps
922 which are hard enough not to sink but sticky, and rocking could help to unstick the limbs
923 (Kuznetsov, 2011). However, the reason may be more profoundly rooted in the primitiveness
924 of the locomotor system of the ancient tetrapods. Two major aspects of this primitiveness

may be thought of. First, the nervous control of the limb muscles possibly was poorly developed, and in this respect, the passive-dynamic locomotion, which relies on the natural-mechanic (automatic) motions of the limbs, is an undoubted advantage. Second, probably there was not much muscular mass developed in the limbs yet, and the efficiency of usage of this mass was more crucial than in the more advanced tetrapods of the later times. Indeed, in the ideal passive-dynamic walker the rigid limbs swing freely and do not need actuators at all, and in the real passive-dynamic walker the power of actuators is only necessary to compensate for energy losses associated mainly with collisions and also with minor forces of friction and drag. In the idealized unbending limbs, there are no unwanted losses due to negative actuator work, which is inevitable if the limb joints bend and extend and which minimization requires advanced coordination (Kuznetsov, 2018). As to the losses associated with collisions, they could be rather small in pareiasaurs, as is shown by the fact that a few children easily compensate these losses when pulling and rocking the 90 kg model from side to side to make it walk. However, as was shown by theoretical 3D analysis (Remy *et al*., 2010b), these collisional energy expenses cannot be considered negligible with the *Sukhonopus*-like wide limb posture.

At the moment, there are two successful, although basically different, reverse-engineering hardware models of walking Paleozoic (Permian) tetrapods – the *Sukhonopus* producer toy (this study) and the *Orobates* robot (Nyakatura *et al*., 2019). Interestingly, the two implementations illustrate two quite opposite sprawling types that were found to exist among tetrapods (Kuznetsov, 1999; Gambaryan & Kuznetsov, 2013). The *Orobates* robot illustrates the classic sprawling type of a lizard with widely spread limbs and low body position, although the belly and tail do not touch the ground. The designers endowed it with an idealized gait known as the slow or walking trot based on the following reasoning in the Supplementary information: "Hands and feet were forced to contact the ground with limb

phase of 0.5, duty factor of 0.75 and a stride frequency of 0.75 Hz – that is, an idealized walking trot (as was occasionally exhibited by all of the extant species that we studied)." This referred to two lizard species, a salamander, and a caiman. In the *Sukhonopus* toy, these parameters are all different: the limbs, although sprawling, are kept closer to the midline supporting the body high above the ground, and the gait is the idealized slow pace with limb phase of 0 and duty factor just a little above 50% (the same as 0.5), which means that all the four feet are on the ground together very briefly. The joint kinematics is also very different in accordance with the aforementioned definition of the two sprawling types (Kuznetsov, 1999; Gambaryan & Kuznetsov, 2013). In the limb contact phase, the *Orobates* robot mainly employs retraction of the limb in the horizontal plane produced by rotation of the humerus or the femur about the vertical axis in the glenoid or acetabulum, respectively. Contrary to that, the *Sukhonopus* toy employs retraction of the limb in the vertical parasagittal plane produced by rotation of the humerus or the femur about the horizontal transverse axis in the glenoid or acetabulum, respectively.

The dominance of stylopodia (humerus and femur) rotation about either vertical or transverse axis implies, and is based on different geometry of the limb articulation with the girdle. For instance, the humeral rotation about the transverse axis, like in the *Sukhonopus* toy, was at first predicted for monotremes based on the peculiar glenoid and humeral head geometry in *Ornithorhynchus* (Howell, 1937a, 1937b), and much later confirmed for all extant genera of monotremes based on cineradiography (Jenkins, 1970; Pridmore, 1985). The monotremes, in contrast to all the other extant mammals, retain the sprawling limb posture, and for the sprawling humerus or femur, the transverse axis of rotation almost coincides with the proper long axis of the bone. Surprisingly, the geometry-restricted nature of glenoid mobility in *Ornithorhynchus* is entirely ignored in recent computer modeling (Pierce *et al*., 2012). Without any apparent reason, these authors approximate the joint by a simple sphere.

975 They write in the Supplementary information: "With respect to the shoulder and hip, spheres
976 were placed in the glenoid and acetabulum to estimate each joint’s centre of rotation,
977 assuming a ball-and-socket (three degrees of freedom) joint." This approximation contradicts
978 the glenoid geometry of *Ornithorhynchus*, and furthermore, it contradicts the glenoid and
979 acetabular geometry of the main subject of Pierce *et al*. (2012), which is the *Ichthyostega*.
980 Not only its glenoid is screw-shaped, which is typical of the lower tetrapods, but its
981 acetabulum is similarly shaped too, which is unique. The screw-shaped glenoid geometry was
982 much debated by earlier workers as indicative of available humeral mobility (*e.g.*, Romer,
983 1922). In recent publications, the kinematical limitations imposed by the screw-shaped
984 glenoid on the humeral mobility are taken into account but rarely (Hopson, 2015). The
985 ancestral "screw shape" is retained in pareiasaurians, although in a much shorter form
986 (Romer, 1922). Apparently, its approximation with a sphere would be an oversimplification.
987 It can be best approximated with the hinge joint, whose axis of rotation passes at right angles
988 (transverse) to the sagittal plane, like it was implemented in the *Sukhonopus* producer pacing
989 model. This direction of the axis of rotation, being more or less aligned with the shaft of the
990 sprawling humerus, is actually observed in monotremes (Jenkins, 1970; Pridmore, 1985), and
991 it was also supposed for *Dimetrodon* (Hopson, 2015).
992 The last point to be highlighted is the hard clattering of the *Sukhonopus* producer model
993 walking on a floor. Definitely, the living pareiasaurians had some paw pads and walked on a
994 softer ground than the floor is. In any case though, when pacing in such a rocking manner
995 associated with collisions, the large and heavy tetrapods should produce loud stomping
996 sounds. If this technique of locomotion was widespread among large barrel-bodied tetrapods
997 who walked on land in the Paleozoic, *e.g.*, herbivorous Diadectomorpha, Caseasauria,
998 Dicynodontia, the relations between predators and prey could probably be mainly mediated
999 by seismic hearing, without the need of sensing the airborne sound. Seismic hearing is a well-

reasoned feature of Paleozoic tetrapods characterized by massive stapes, which is inappropriate to transmit airborne sound (Tumarkin, 1955, 1968). Possibly, one of the major inventions of tetrapods at the Paleozoic-to-Mesozoic transition was the softer non-rocking terrestrial locomotion. If so, the explosive evolution of hearing the airborne sounds in a wide variety of tetrapod taxa at this transition (Tumarkin, 1955, 1968; Senter, 2008) may be inferred as the response to this change of the basic type of quadrupedal locomotion.

CONCLUSIONS

Pareiasaurians were probably specialized in terrestrial locomotion of a very peculiar type unusual among the extant tetrapods. It is hypothesized that the passive-dynamic rocking pace of pareiasaurs, and possibly of some other Paleozoic tetrapods, proved feasible by the natural-sized kinetic model of the *Sukhonopus* producer, was associated with deficiency of nervous and muscular supply of the limbs and, indirectly, with deficiency of sensing the airborne sound. The ichnological indicator of this locomotion technique is the inward turn of the forelimb footprints, and the histological indicator is the extensive development in the long limb elements of spongy bone tissue in place of the marrow cavity and superficial compact layer, which becomes especially reduced on the inner side. The other probable indicators of the rocking pace-like walk are trackway narrowness associated with increased footprint angulation (up to 140^0 in the trackway described by Smith, 1993), the horizontal (tangential) orientation of presacral zygapophyseal articular facets manifesting the enlarged range of axial twisting of the spine, and the barrel-shaped skeleton of the rib cage which manifests restricted lateral bending of the spine. The screw-shaped glenoid known since the earliest tetrapods is indicative of the dominance of the humeral axial rotation in the shoulder joint (Hopson, 2015). This kind of mobility is the prerequisite for the development of the narrow variant of

the sprawling posture, on which the rocking pace is based (Kuznetsov, 1999; Gambaryan & Kuznetsov, 2013).

ACKNOWLEDGMENTS

I studied the trackway of the Strel´na River in 2006 as a guest of the expedition of the Borissiak Paleontological Institute led by V. K. Golubev. I am grateful for the support to all members of the expedition, and especially to the late Yu. M. Gubin for his wise advice to concentrate on the longest and the best trackway (here referred to as the trackway L) of a number which were available nearby. A. A. Kurkin helped me in the field and also in measuring *Deltavjatia* skeletons, and introduced me to A. L. Toropov. Due to the hospitality of A. L. Toropov and his staff, I measured the skeletons of *Deltavjatia* at the Vyatka Palaeontological Museum in 2011. The photo on Fig. 5.1 was shot by A. L. Toropov in 2020 on my special request. E. I. Boyarinova kindly shared many photos of *Deltavjatia*.

I designed the hardware model of a walking pareiasaur and the scenario for the lesson with this model under the inspiration of I. A. Kolmanovsky, former Head of the Biological Laboratory of the Polytechnic Museum, which funded implementation of the whole project. The skin envelope for the model was created by the professional sculptor E. S. Kuznetsova. A. A. Panyutina helped me mount the metal frame inside the skin envelope and assisted E. S. Kuznetsova in the skin painting. N. E. Prilepskaya scanned the trackway S in the Orlov Paleontological Museum of the Borissiak Paleontological Institute. The reviewers of the manuscript suggested a number of important content improvements. D. T. Razmadze, A. A. Repin, and the reviewers made corrections to my English text.

The trackway analysis and manuscript writing were supported by the Russian Foundation for Basic Research grants 17-04-00954 and 20-04-00357.

1049 LITERATURE CITED

1050 Ahlberg, P. E., Clack, J. A., and Blom, H. 2005. The axial skeleton of the Devonian
1051 tetrapod *Ichthyostega*. *Nature* 437 (7055): 137–140.
1052 Alexander, R. McN. 1989. *Dynamics of Dinosaurs and Other Extinct Giants.* Columbia
1053 University Press.
1054 Alexander, R. McN., 1995. *How animals move*. CD-ROM. Ed.: Kuznetsov, A. The
1055 Discovery Channel and Maris Multimedia.
1056 Baird, D. 1952. Revision of the Pennsylvanian and Permian footprints *Limnopus*,
1057 *Allopus* and *Baropus*. *Journal of Paleontology* 26 (5): 832–840.
1058 Boitsova, E. A., Skutschas, P. P., Sennikov, A. G., Golubev, V. K., Masuytin, V. V.,
1059 and Masuytina, O. A. 2019. Bone histology of two pareiasaurs from Russia (*Deltavjatia*
1060 *rossica* and *Scutosaurus karpinskii*) with implications for pareiasaurian palaeobiology.
1061 *Biological Journal of the Linnean Society* 128 (2): 289–310.
1062 Brand, L. R., and Tang, T. 1991. Fossil vertebrate footprints in the Coconino Sandstone
1063 (Permian) of northern Arizona: evidence for underwater origin. *Geology* 19 (12): 1201–1204.
1064 Canoville, A., and Chinsamy, A. 2017. Bone Microstructure of Pareiasaurs
1065 (Parareptilia) from the Karoo Basin, South Africa: Implications for Growth Strategies and
1066 Lifestyle Habits. *The Anatomical Record* 300 (6): 1039–1066.
1067 Canoville, A., Thomas, D. B., and Chinsamy, A. 2014. Insights into the habitat of
1068 Middle Permian pareiasaurs (Parareptilia) from preliminary isotopic analyses. *Lethaia* 47 (2):
1069 266–274.
1070 Cartmill, M., Lemelin, P., and Schmitt, D. 2002. Support polygons and symmetrical
1071 gaits in mammals. *Zoological Journal of the Linnean Society* 136 (3): 401–420.
1072 Clack, J. A. 1997. Devonian tetrapod trackways and trackmakers; a review of the
1073 fossils and footprints. *Palaeogeography, Palaeoclimatology, Palaeoecology* 130: 227–250.

1074 Daeschler, E. B., Shubin, N. H., and Jenkins, F. A., Jr. 2006. A Devonian tetrapod-like
1075 fish and the evolution of the tetrapod body plan. *Nature* 440 (7085): 757–763.
1076 Gambaryan, P. P., and Kuznetsov, A. N. 2013. An evolutionary perspective on the
1077 walking gait of the long-beaked echidna. *Journal of Zoology* 290 (1): 58–67.
1078 Gray, J. 1944. Studies in the mechanics of the tetrapod skeleton. *Journal of*
1079 *Experimental Biology* 20 (2): 88–116.
1080 Gregersen, G.G., and Lucas, D.B. 1967. An in vivo study of the axial rotation of the
1081 human thoracolumbar spine. *The Journal of Bone & Joint Surgery* 49 (2): 247–262.
1082 Gregory, W. K. 1951. *Evolution Emerging*, 2 volumes. The MacMillan Company, New
1083 York, 1013 p.
1084 Gubin, Y. M., Golubev, V. K., Bulanov, V. V., and Petuchov, S. V. 2003. Pareiasaurian
1085 tracks from the upper Permian of Eastern Europe. *Paleontological Journal* 37 (5): 514–523.
1086 Hildebrand, M. 1965. Symmetrical gaits of horses. *Science* 150: 701–708.
1087 Hildebrand, M. 1966. Analysis of the symmetrical gaits of tetrapods. *Folia*
1088 *Biotheoretica* 6: 9–22.
1089 Hildebrand, M. 1967. Symmetrical gaits of primates. *American Journal of Physical*
1090 *Anthropology* 26: 119–130.
1091 Hildebrand, M. 1968. Symmetrical gaits of dogs in relation to body build. *Journal of*
1092 *Morphology* 124: 353–360.
1093 Hildebrand, M. 1977. Analysis of asymmetrical gaits. *Journal of Mammalogy* 58 (2):
1094 131–156.
1095 Hildebrand, M. 1989. The quadrupedal gaits of vertebrates. *BioScience* 39: 766–775.
1096 Hopson, J. A. 2015. Fossils, trackways, and transitions in locomotion: a case study of
1097 *Dimetrodon*. In: Dial, K. P, Shubin, N., and Brainerd, E. L. (Eds.), *Great transformations in*
1098 *vertebrate evolution*, p. 125–141.

1099 Howell, A. B. 1937a. The swimming mechanism of the platypus. *Journal of*
1100 *Mammalogy* 18 (2): 217–222.
1101 Howell, A. B. 1937b. Morphogenesis of the shoulder architecture. Part V.
1102 Monotremata. *The Quarterly Review of Biology* 12 (2): 191–205.
1103 Howell, A. B. 1944. *Speed in animals, their specialization for running and leaping.*
1104 University of Chicago Press, Chicago.
1105 Jenkins, F. A., Jr. 1970. Limb movements in monotremes (*Tachyglossus aculeatus*): a
1106 cineradiographic analysis. *Science* 168: 1473–1475.
1107 Jones, K. E., Gonzalez, S., Angielczyk, K. D., and Pierce, S. E. 2020. Regionalization
1108 of the axial skeleton predates functional adaptation in the forerunners of mammals. *Nature*
1109 *ecology & evolution* 4: 470–478.
1110 Kienapfel, K., Läbe, S., and Preuschoft, H. 2014. Do tracks yield reliable information
1111 on gaits?–Part 1: The case of horses. *Fossil Record* 17: 59–67.
1112 Kuznetsov, A. N. 1999. Structural types of limbs and evolution of running technique in
1113 tetrapods. *Zoologicheskie Issledovania* 3: 1–94. [in Russian].
1114 Kuznetsov, A. N. 2011. The gaits of certain in-fingered tetrapods. *Ameghiniana* 48: 4
1115 (R): Suplemento Resúmenes, R56.
1116 Kuznetsov, A. N. 2018. A theorem of target points for the ground reaction force in a
1117 planar serial-linked walking limb. *Bioinspiration & Biomimetics* 13 (6): 066010.
1118 Lee, S., and Liu, Y. 2012. Curved glide-reflection symmetry detection. *IEEE*
1119 *transactions on pattern analysis and machine intelligence* 34 (2): 266–278.
1120 Loope, D. B. 1992. Fossil vertebrate footprints in the Coconino Sandstone (Permian) of
1121 northern Arizona: evidence for underwater origin. Comment. *Geology* 20 (7): 667–668.
1122 Lucas, S. G. 2015. *Thinopus* and a critical review of Devonian tetrapod footprints.
1123 *Ichnos* 22: 136–154.

1124 Marchetti, L., Voigt, S., and Klein, H. 2017. Revision of Late Permian tetrapod tracks
1125 from the Dolomites (Trentino-Alto Adige, Italy). *Historical Biology* 31 (6): 748–783.
1126 Martino, R. L. 1991. *Limnopus* trackways from the Conemaugh Group (Late
1127 Pennsylvanian), southern West Virginia. *Journal of Paleontology* 65 (6): 957–972.
1128 Niedźwiedzki, G., Szrek, P., Narkiewicz, K., Narkiewicz, M., and Ahlberg, P. E. 2010.
1129 Tetrapod trackways from the early Middle Devonian period of Poland. *Nature* 463 (7277):
1130 43–48.
1131 Nyakatura, J. A., Melo, K., Horvat, T., Karakasiliotis, K., Allen, V. R., Andikfar, A.,
1132 Andrada, E., Arnold, P., Lauströer, J., Hutchinson, J. R., Fischer, M. S., and Ijspeert, A. J.
1133 2019. Reverse-engineering the locomotion of a stem amniote. *Nature* 565 (7739): 351–355.
1134 Padian, K., and Olsen, P. E. 1984. Footprints of the Komodo monitor and the trackways
1135 of fossil reptiles. *Copeia*: 662–671.
1136 Peabody, F. E. 1959. Trackways of living and fossil salamanders. *University of*
1137 *California Publications in Zoology* 63 (1): 1–72. University of California Press.
1138 Pierce, S. E., Clack, J. A., and Hutchinson, J. R. 2012. Three-dimensional limb joint
1139 mobility in the early tetrapod *Ichthyostega*. *Nature* 486 (7404): 523–526.
1140 Pridmore, P. A. 1985. Terrestrial locomotion in monotremes (Mammalia:
1141 Monotremata). *Journal of Zoology* 205: 53–73.
1142 Rautian, A. S. 2002. Features of locomotion of a big reptile, which produced trackways
1143 on the Late Permian sediment exposures of the Sukhona and Strel´na rivers (Vologda region).
1144 In: L. P. Tatarinov, and Golubev, V. K. (Eds.), *Materials of the 4th Russian conference*
1145 *"Paleontology and Stratigraphy of Permian and Triassic of Northern Eurasia*.
1146 Paleontological Institute, Russian Academy of Sciences, Moscow, p. 83–84. [in Russian].

1147 Remy, C. D., Buffinton, K., and Siegwart, R. 2010a. Stability analysis of passive
1148 dynamic walking of quadrupeds. *The International Journal of Robotics Research* 29 (9):
1149 1173–1185.
1150 Remy, C. D., Hutter, M., and Siegwart, R. 2010b. Passive dynamic walking with
1151 quadrupeds – extensions towards 3D. *2010 IEEE International Conference on Robotics and*
1152 *Automation* 5231–5236.
1153 Rockwell, H., Evans, F.G., and Pheasant, H.C. 1938. The comparative morphology of
1154 the vertebrate spinal column. Its form as related to function. *Journal of Morphology* 63 (1):
1155 87–117.
1156 Romer, A. S. 1922. The locomotor apparatus of certain primitive and mammal-like
1157 reptiles. *Bulletin of American Museum of Natural History* 46: 517–606.
1158 Ruina, A., Bertram, J. E., and Srinivasan, M. 2005. A collisional model of the energetic
1159 cost of support work qualitatively explains leg sequencing in walking and galloping, pseudo-
1160 elastic leg behavior in running and the walk-to-run transition. *Journal of Theoretical Biology*
1161 237 (2): 170–192.
1162 Sellers, W. I., Manning, P. L., Lyson, T., Stevens, K., and Margetts, L. 2009. Virtual
1163 palaeontology: gait reconstruction of extinct vertebrates using high performance computing.
1164 *Palaeontologia Electronica* 12 (3): 11A: 26p.
1165 Senter, P. 2008. Voices of the past: a review of Paleozoic and Mesozoic animal sounds.
1166 *Historical Biology* 20 (4): 255–287.
1167 Smith, A. C., and Berkemeier, M. D. 1997. Passive dynamic quadrupedal walking.
1168 *Proceedings of the 1997 IEEE International Conference on Robotics and Automation* 1: 34–
1169 39.
1170 Smith, R. M. 1993. Sedimentology and ichnology of floodplain paleosurfaces in the
1171 Beaufort Group (Late Permian), Karoo sequence, South Africa. *Palaios* 8 (4): 339–357.

1172 Sukhanov, V. B. 1963. Forms of movement (gaits) of land vertebrates (a theory of
1173 locomotion and of the evolution of its forms). *Bulletin of the Moscow Society of Naturalists*
1174 68 (5): 136–137. [in Russian].
1175 Sukhanov, V. B. 1967. Data on the locomotion of land vertebrates. 1. General
1176 classification of symmetrical gaits. *Bulletin of the Moscow Society of Naturalists* 72 (2): 118–
1177 135. [in Russian].
1178 Sukhanov, V. B. 1968. General system of symmetrical locomotion of terrestrial
1179 vertebrates and some features of movement of lower tetrapods. Leningrad: Nauka. [in
1180 Russian].
1181 Sukhanov, V. B. 1974. *General system of symmetrical locomotion of terrestrial*
1182 *vertebrates and some features of movement of lower tetrapods* (translated by M. M. Hague).
1183 New Delhi: Amerind Publishing Co. Pvt. Ltd.
1184 Thompson, M. E., White, R. S., and Morgan, G. S. 2007. Pace versus trot: can medium
1185 speed gait be determined from fossil trackways. *Cenozoic vertebrate tracks and traces: New*
1186 *Mexico Museum of Natural History & Science Bulletin* 42: 309–314.
1187 Thorp, B. H., and Dixon, J. M. 1991. Cartilaginous bone extremities of growing
1188 monotremes appear unique. *The Anatomical Record* 229 (4): 447–452.
1189 Triggs, B. 2003. *Tracks, Scats and Other Traces: a Field Guide to Australian*
1190 *Mammals*. Oxford Univ. Press. 340 p.
1191 Tumarkin, A. 1955. On the evolution of the auditory conducting apparatus: a new
1192 theory based on functional considerations. *Evolution* 9 (3): 221–243.
1193 Tumarkin, A. 1968. Evolution of the auditory conducting apparatus in terrestrial
1194 vertebrates. *Ciba Foundation Symposium – Hearing Mechanisms in Vertebrates*. Chichester,
1195 UK: John Wiley & Sons, Ltd. p. 18–40.

1196 Valentini, M., Conti, M. A., and Nicosia, U. 2008. Linking tetrapod tracks to the
1197 biodynamics, paleobiogeography, and paleobiology of their trackmakers: *Pachypes*
1198 *dolomiticus* Leonardi et al., 1975, a case study. *Acta Geologica* 83: 237–246.
1199 Valentini, M., Nicosia, U., and Conti, M. A. 2009. A re-evaluation of *Pachypes*, a
1200 pareiasaurian track from the Late Permian. *Neues Jahrbuch für Geologie und Paläontologie-*
1201 *Abhandlungen* 251 (1): 71–94.
1202 Warren, J. W., and Wakefield, N. A. 1972. Trackways of tetrapod vertebrates from the
1203 Upper Devonian of Victoria, Australia. *Nature* 238 (5365): 469–470.
1204

1205 TABLES

1206 Table 1. Estimates of glenoacetabular lengths in centimeters and pes lengths for two
1207 trackways included in the ichnogenus *Sukhonopus* based on different trot and pace
1208 presumptions (cf. Fig. 3 and Supplementary material 2 row 5). The left column represents the
1209 reference points for every analysis

			long pacer	long trotter	middle pacer	short trotter	short pacer
trackway S	n (sample size)		0	1	2	3	4
manus dig.III pes digit III	cm	mean	N/A	150.0	106.8	65.5	22.8
	pes lengths	mean	N/A	9.68	6.89	4.23	1.47
trackway L	n (sample size)		26	27	28	29	30
Analysis A: pes digit III manus dig.III	cm	mean	245.6	192.9	140.2	87.6	35.0
		SD	7.8	5.2	3.5	4.3	5.4
	pes lengths	mean	12.29	9.65	7.01	4.38	1.75
		SD	0.39	0.26	0.18	0.21	0.27
Analysis B: pes digit IV manus dig.III	cm	mean	242.6	189.8	137.1	84.6	32.1
		SD	8.1	5.5	3.9	4.6	5.7
	pes lengths	mean	12.13	9.50	6.86	4.23	1.61
		SD	0.41	0.28	0.19	0.23	0.29
Analysis C: rough centers	cm	mean	246.1	193.1	140.3	87.6	35.0
		SD	8.2	5.7	4.0	4.4	5.6
	pes lengths	mean	12.31	9.66	7.02	4.38	1.75

1210

1211 Table 2. Measurements and proportions of the glenoacetabular (gl-ac) and pes lengths
1212 in four skeletons of *Deltavjatia rossica* from the Vyatka Palaeontological Museum

specimen	gl-ac length (cm)	pes length (cm)	gl-ac to pes ratio
KPM 232	81.0	right 10	8.10
KPM 234	71.5	right 10	7.15
KPM 289	70.5	left 12	5.88
KPM 290	79.5	right 13	6.12

1213

FIGURES

FIGURE 1. Shapes of selected footprints from the trackway *Sukhonopus*, specimens S (column A) and L (columns B–E) shown to the same scale. The travel direction is from the left to the right. Row 1 – left forelimb, row 2 – right forelimb, row 3 – left hindlimb, row 4 – right hindlimb. Column A – the 1st left manus imprint, the 3rd right manus imprint, the 2nd left pes imprint, and the 3rd right pes imprint of the trackway S 3D scan (Supplementary material 1). Column B – the 9th left manus imprint, the 11th right manus imprint, the 16th left pes imprint, and the 12th right pes imprint of the trackway L photo panorama (Supplementary material 2). Column C – the same as the column B with the footprint outlines. Column D – on the images 1 and 3 the paired outlines from the column C are combined to obtain the averaged outlines (black) which are represented alone on the images 2 and 4 of the column. Column E – the same as the column C with the averaged outlines instead of the specific ones.

FIGURE 2. Photo panorama of the last 2.5 strides of the trackway L (the same number of strides as on the complete trackway S represented in Supplementary material 1). The travel direction is from the left to the right. For scale and geometric purposes, the rope grid is put on the trackway having 25x25 cm cells and a wooden frame, which corners are loaded with stones, because rather fast and about 20 cm deep water flow passes over (from the top to the bottom of the figure). The white areas are foam patches on the river surface. The panorama is composed of 6 successive photos which were corrected regarding distortion. After the corrections, they were joined together automatically by means of Adobe Photoshop panorama function. The accuracy of the method is about 10 mm as can be seen by rope mismatches at the photos' junctions. The best left pes imprint selected for Fig. 1 is highlighted by blue rectangle.

FIGURE 3. Footprint map of the last part of trackway L shown on Fig. 2. The travel direction is from the left to the right. The manus imprints are pink and the pes imprints are pale blue. The length of the best pes imprint is shown by the horizontal blue bar of 20 cm length. The red segment is drawn between the digit III tips of the last pair of the manual imprints. The middle of this segment shown as the green dot serves as the starting point to measure the glenoacetabular length; the last is measured from this point backwards as is indicated by the magenta arrow. The glenoacetabular length is measured in pes lengths indicated by the repeated blue bars over the magenta arrow. The blue zigzag line is drawn through the digit III tips of successive pedal imprints (this corresponds to analysis A in Table 1). Every segment of the zigzag line represents position of the two hind feet when both of them are placed in respective footprints. The yellow dot placed in the middle of each blue segment represents the respective position of mid-sagittal point between the left and right acetabula. Above the trackway map, the Hildebrand-Sukhanov chart of symmetrical gaits is spread repeatedly. The vertical lines of trot and pace on the chart are aligned with appropriate yellow dots of the blue zigzag on the footprint map. The dark grey area on the chart represents the gaits of extant reptiles according to Sukhanov (1968, 1974), the wider pale grey area (with the reptilian area included) represents the mammalian symmetrical gaits according to Hildebrand (1968, 1989), and the dotted stripe represents the gait of the long-beaked echidna according to Gambaryan & Kuznetsov (2013). The lower series of yellow arrowheads is a plot of acetabula positions in four skeletons of *Deltavjatia rossica* (Table 2) relative to glenoid (green dot) on the glenoacetabular axis (magenta arrow); the upper reversed arrowheads point on respective limb-phase values on the gait chart.

FIGURE 4. Statistical representation of different pacers' and trotters' glenoacetabular length stability throughout trackway L based on data from Table 1, aligned with the limb-

phase axis of the Hildebrand-Sukhanov chart of symmetrical gaits. Red arrow indicates relation of the binomial approximation minimum of the plot to the chart. See the chart explanation on Fig. 3 and plot explanation in the text.

FIGURE 5. Pes length in *Deltavjatia rossica* measured as is shown by blue arrows, between the distal border of the astragalus and the digit III tip. Dorsal view. 1, left hindlimb of the best preserved specimen KPM 289 (photo by V. V. Bulanov). 2, right hindlimb of the specimen KPM 232 cast (photo by A. L. Toropov). In KPM 232 the digital phalanges look unnaturally reduced in length as compared to those of KPM 289.

FIGURE 6. *Deltavjatia rossica* specimen KPM 289 represents a complete naturally articulated 3D-preserved skeleton showing the inward turn (red arrow) of the manus. Photo by E. I. Boyarinova.

FIGURE 7. The natural-sized model of the *Sukhonopus* producer is pacing being driven forward by children and pushed from side to side by I. A. Kolmanovsky. The ease of their labor is obviously visible; three children pull the rope together for fun, actually one could manage. At the moment, the model is rocked to the left side, the left limbs are supporting the body, and the right ones are swinging forward. The glenoid hinge axis of rotation is indicated by the green dot, the acetabulum hinge axis of rotation – by the yellow dot; actually both axes are transverse to the sagittal plane of the model. The glenoacetabular length is indicated for scale.

FIGURE 8. *Deltavjatia rossica* specimen KPM 286 representing the inward-turned left manus shaped similarly to the outlines of the manual imprints of *Sukhonopus* (copied from

Fig. 1). Dorsal view; the skull is temporarily taken away from the mandible. Photo by E. A. Boitsova.

FIGURE 9. The presumed force distribution in a rocking pacer when it rocks (big pale arrow) from the left limbs to the right ones; anterior view. The right limbs hit the ground with a burst of ground reaction force (blue vector) acting along the limb towards its proximal hinge (yellow flash); the impact is apparently harder in the hindlimb. The left limbs, before leaving the ground, produce active push on the body towards the right side; the ground reaction force (red vector) is declined from the long axis of these limbs towards the common center of mass (CoM) of the body due to contraction of the abductor muscles (*e.g.*, m. dorsalis scapulae) at the proximal hinge (yellow dot); the push of the forelimb is apparently more powerful. In the elbow and knee joints, the outer ligaments (cyan stripes) are subjected to tension. The force diagram is drawn on the photo of the sculptor E. S. Kuznetsova working on the clay prototype of the walking model of the *Sukhonopus* producer.

FIGURE 10. Russian kinetic toy called a "walking-rocking bull-calf" modified for four-beat walking by cutting its trunk into halves and introducing an additional degree of freedom between the halves corresponding to axial rotation of the spine found in echidnas. The spine hinge axis of rotation is indicated by the white line, the glenoid hinge axis of rotation – by the green line, the acetabular hinge axis of rotation – by the yellow line. The glenoacetabular length is indicated for scale. Photo by S. V. Fomin.

FIGURE 11. Presacral vertebrae of *Deltavjatia rossica* specimen KPM 289 in posterior view. The tangential (horizontal) orientation of the articular facets of zygapophyses shown by arrows facilitates the axial rotation in the spine.

SUPPLEMENTARY MATERIALS

SUPPLEMENTARY MATERIAL 1. Surface of *Sukhonopus*, trackway S (stored in the Borissiak Paleontological Institute as PIN 4850/4 and exhibited in the Orlov Paleontological Museum) scanned with Artec Eva 3D scanner and processed in Artec Studio Professional Software.

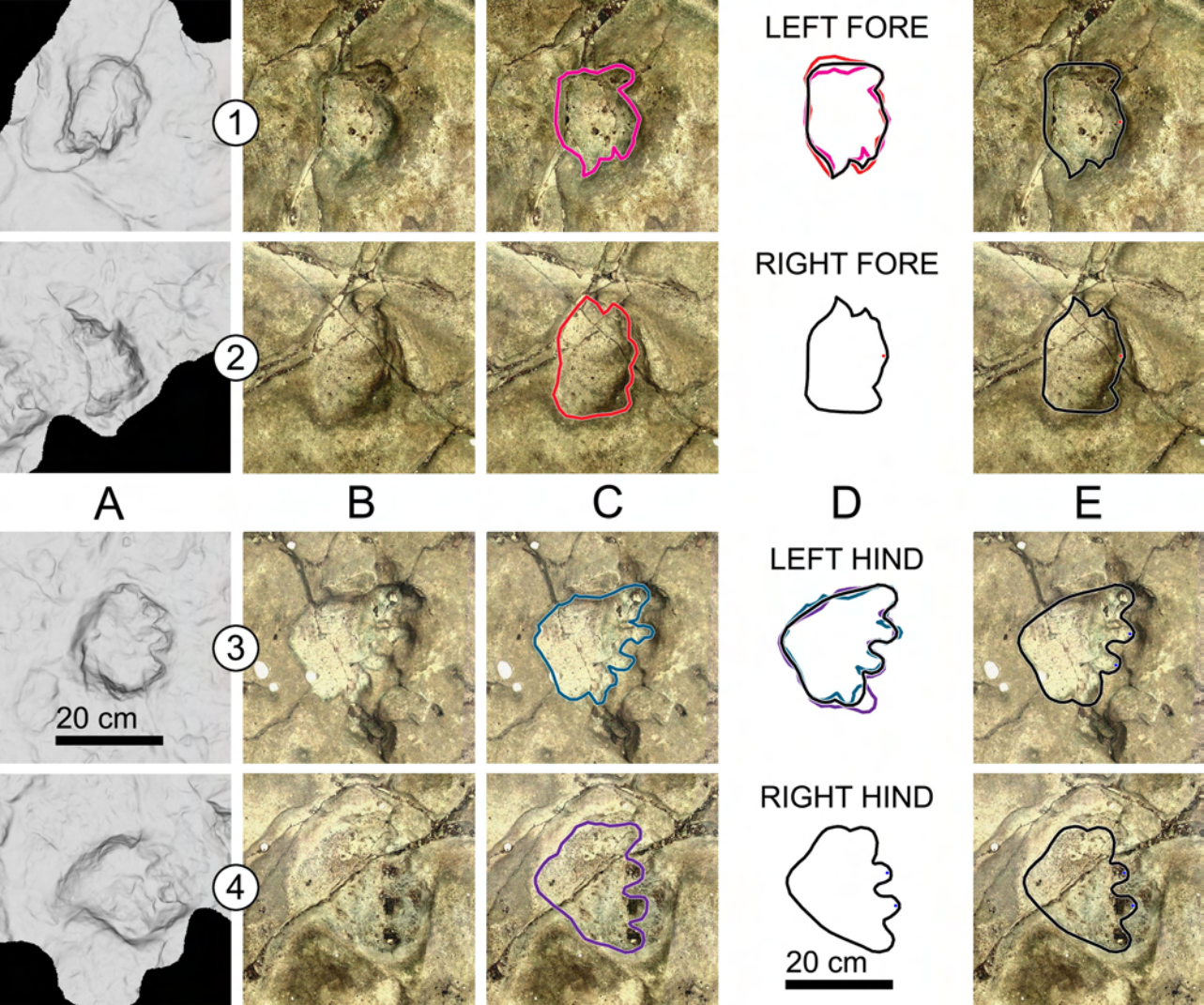
SUPPLEMENTARY MATERIAL 2. Photo panorama of the complete trackway L (*Sukhonopus* from the Strel´na River); it is half-size of the original which was actually used in statistical analyses A and B (see the main text). The travel direction is from the left to the right. 1 – panorama with a series of frames with a rope grid of 25x25 cm (the last frame at the right corresponds to Fig. 2 in the main text). 2 – clean panorama without the grid frames (coloration difference from 1 is due to different lighting conditions which are crucial when taking photos through a water layer). 3 – the same as 2 with footprint outlines; the best footprints used on Fig. 1 in the main text are highlighted by coloured outlines, red for the manual imprints and blue for the pedal ones. 4 – footprint map with additional geometric construction for analysis A (see the main text); the red zigzag is drawn through digit III tips of successive manual footprints, and the green dot placed in the middle of each red segment represents the respective position of mid-sagittal point between the left and right glenoids; the blue zigzag with the yellow dots represents the same for the hindlimb with the footprint reference points at the digit III tips. 5 – the same as 3 with the schemes of five possible trackmakers considered in the main text (Table 1 therein), from the left to the right: long pacer, long trotter, middle pacer (most probable), short trotter (corresponding to Baird, 1952), short pacer.

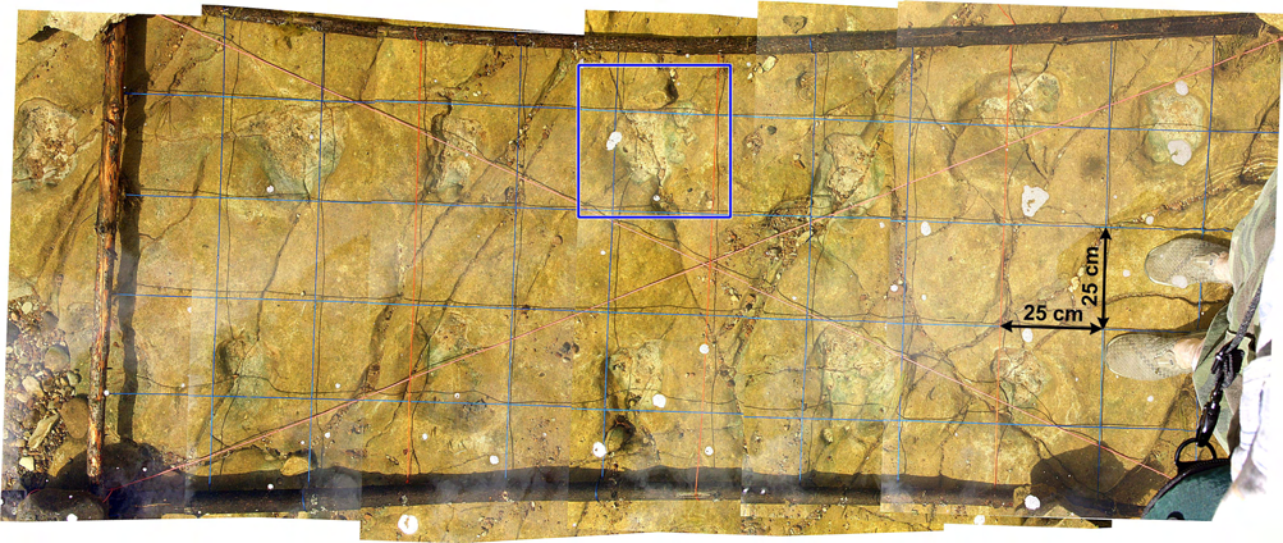
SUPPLEMENTARY MATERIAL 3. Video recording of the traditional Russian kinetic toy called a "walking-rocking bull-calf" going down a shallow-inclined plank. The body mass of the toy is 51 g.

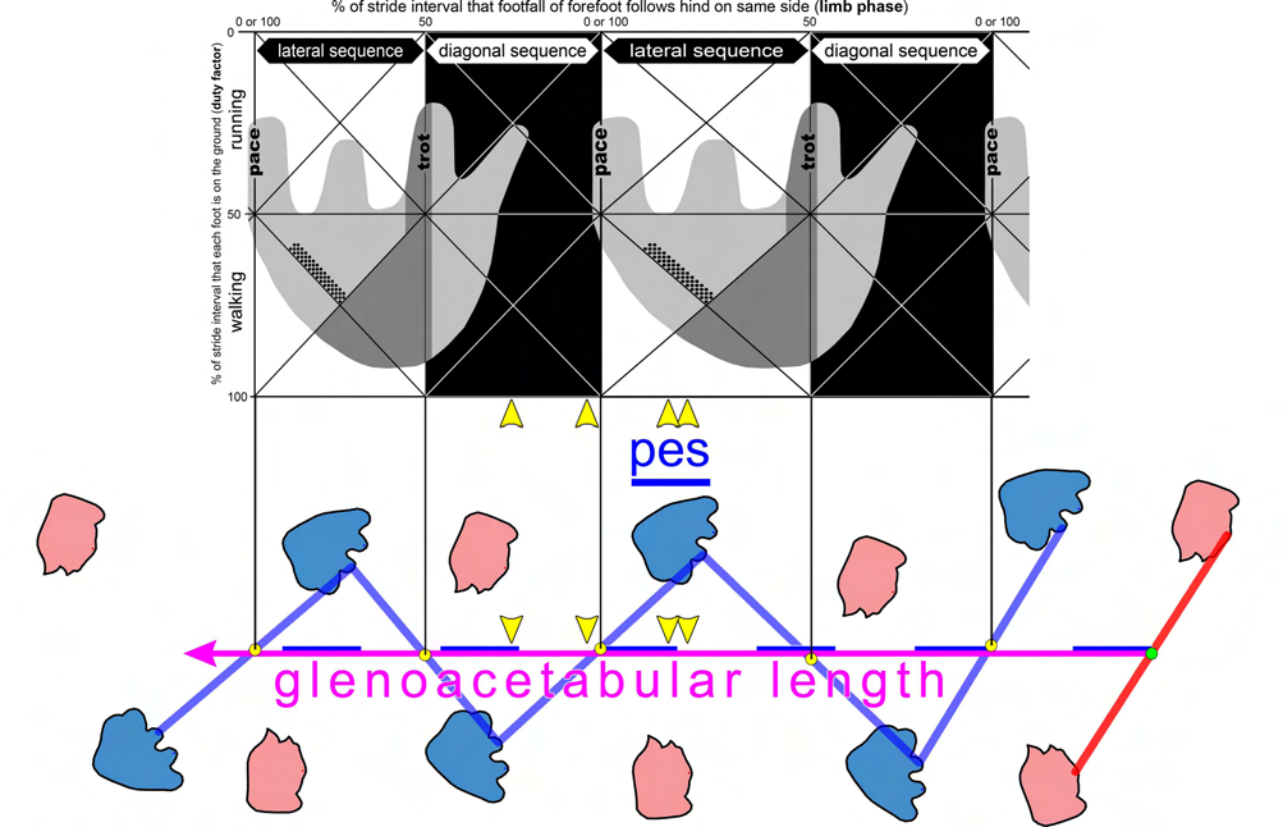
SUPPLEMENTARY MATERIAL 4. One of the first video recordings of the natural-sized pacing model of the *Sukhonopus* producer. Note the limb stomping sounds.

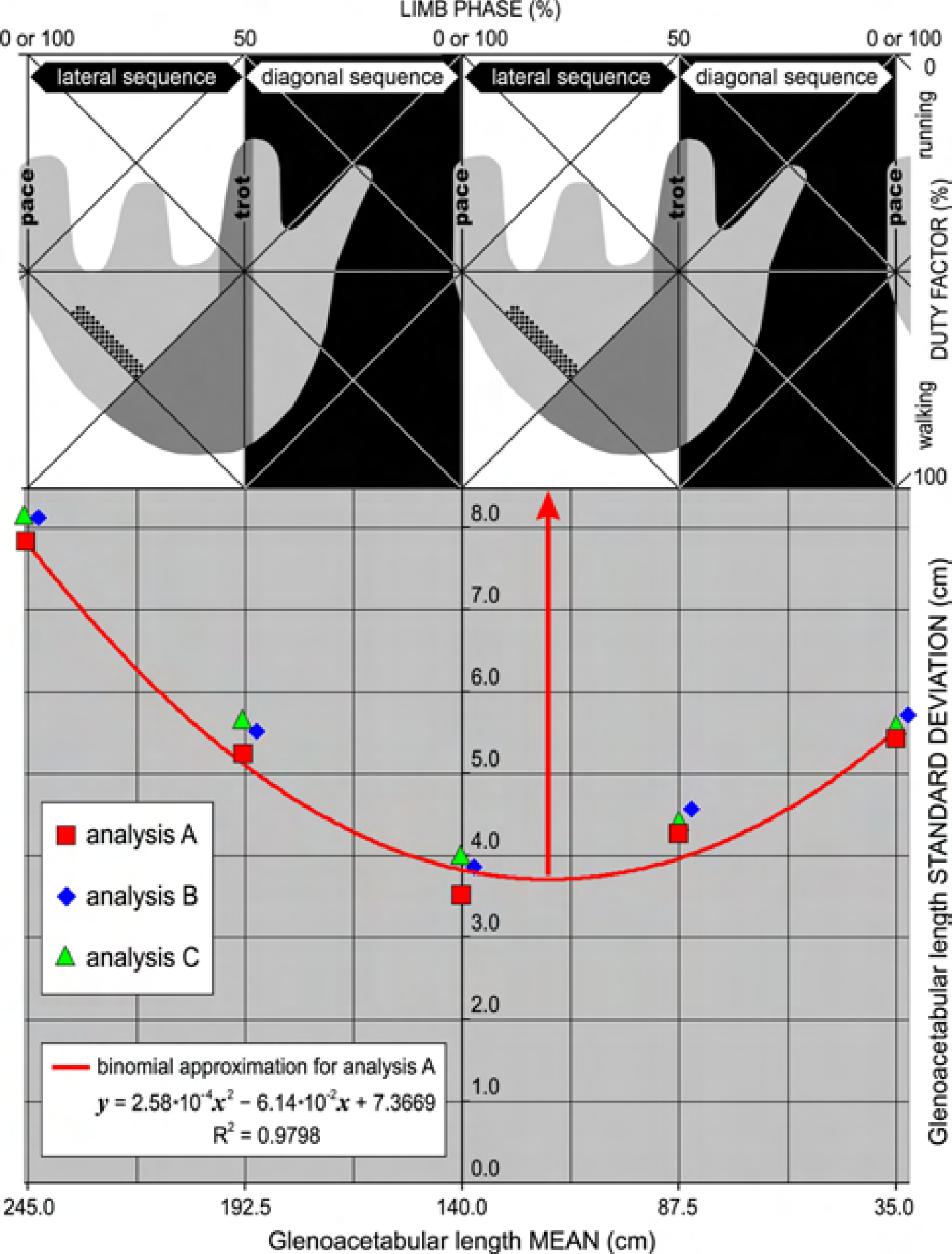
SUPPLEMENTARY MATERIAL 5. Video recording of the modified version of the walking-rocking bull-calf toy enabled for four-beat walking by cutting the trunk into halves and rejoining them via a spinal hinge with the longitudinal axis of rotation. It goes over a horizontal table, being pulled by the weight on a thread kinking over the table edge. The body mass of the toy is 57 g; the weight on the thread pulling the toy to the table edge is 5 g. Due to the additional degree of freedom in the spine, the gait of the modified toy is shifted a little from the exact pace (which is the gait of the non-modified bull-calf toy as well as of the pareiasaur model) to the area of the pace-like lateral-sequence walk (which is the gait of echidnas reported by Gambaryan, Kuznetsov, 2013). The decoupled ground-hitting sounds of the ipsilateral fore and hind limbs can be heard at playback. The modified toy covers the distance of 49 cm in 23 strides during 12 seconds.

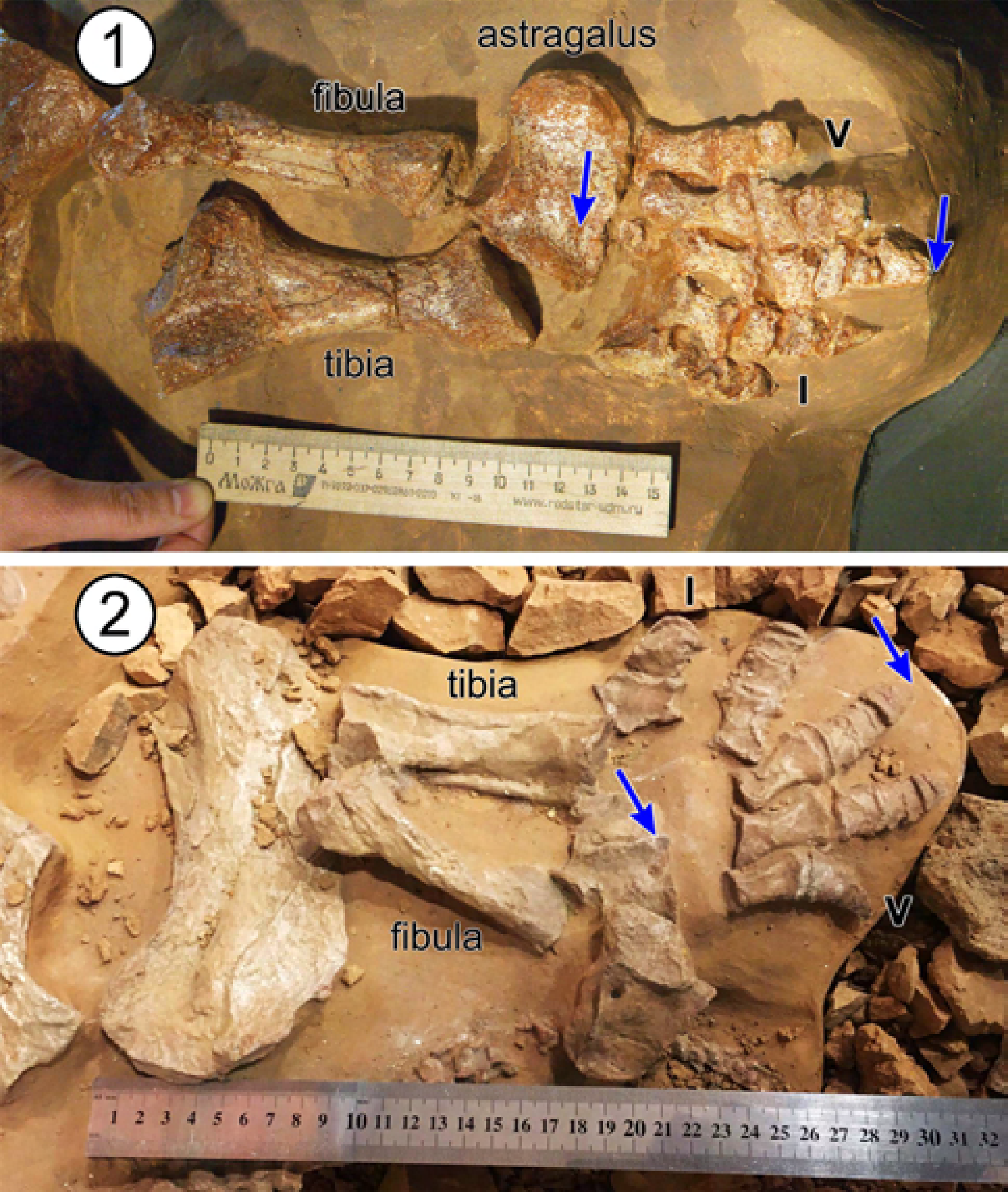
SUPPLEMENTARY MATERIAL 6. Control for Supplementary material 5. The modified walking-rocking bull-calf toy is returned to its original state by blocking the mobility in the spinal hinge with the help of a brace on the belly binding the two trunk halves. The toy covers the distance of 49 cm in 34 strides during 17 seconds.


LEFT FORE
RIGHT FORE
LEFT HIND
RIGHT HIND
1
2
3
4
A
B
C
D
E
20 cm
20 cm


25 cm
25 cm

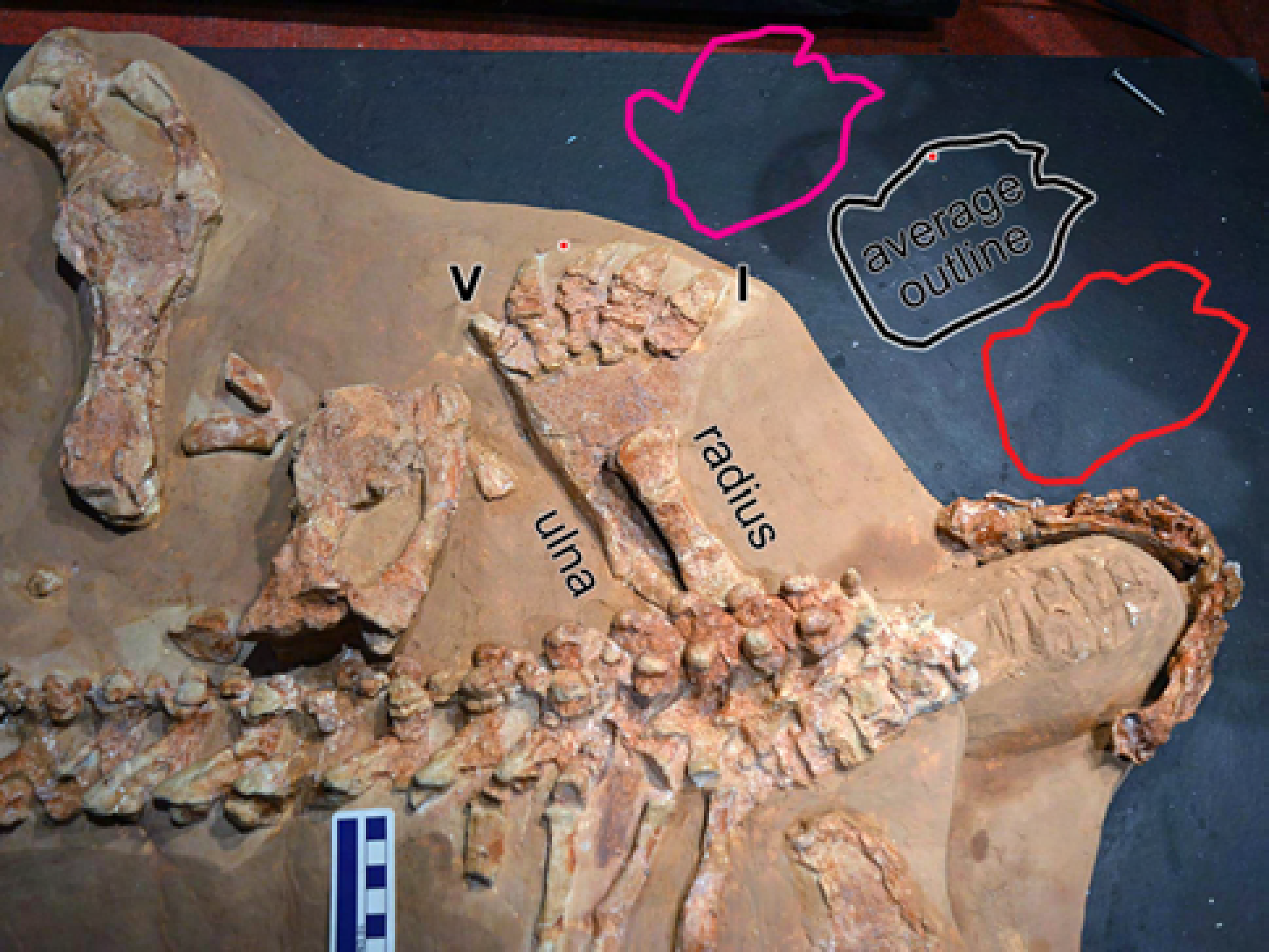

% of stride interval that footfall of forefoot follows hind on same side (limb phase)
0 or 100
50
0 or 100
50
0 or 100
% of stride interval that each foot is on the ground (duty factor)
0
50
100
lateral sequence
diagonal sequence
lateral sequence
diagonal sequence
running
walking
pace
trot
pace
trot
pace
pes
glenoacetabular length

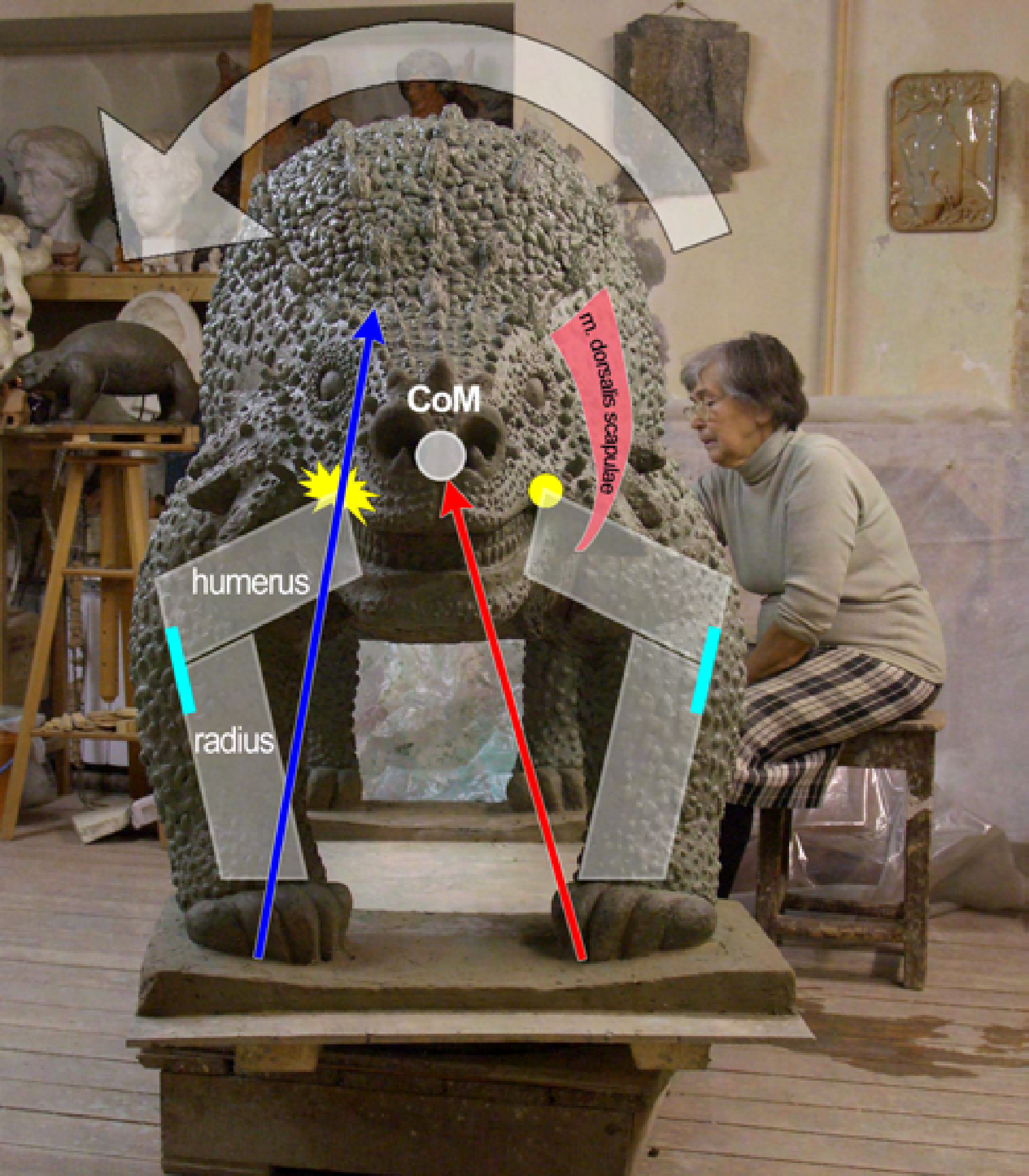

LIMB PHASE (%)
0 or 100
50
0 or 100
50
0 or 100
lateral sequence
diagonal sequence
lateral sequence
diagonal sequence
pace
trot
pace
trot
pace
0
running
DUTY FACTOR (%)
walking
100
8.0
7.0
6.0
5.0
4.0
3.0
2.0
1.0
0.0
Glenoacetabular length STANDARD DEVIATION (cm)
analysis A
analysis B
analysis C
binomial approximation for analysis A
y = 2.58·10-4x2 − 6.14·10-2x + 7.3669
R2 = 0.9798
245.0
192.5
140.0
87.5
35.0
Glenoacetabular length MEAN (cm)

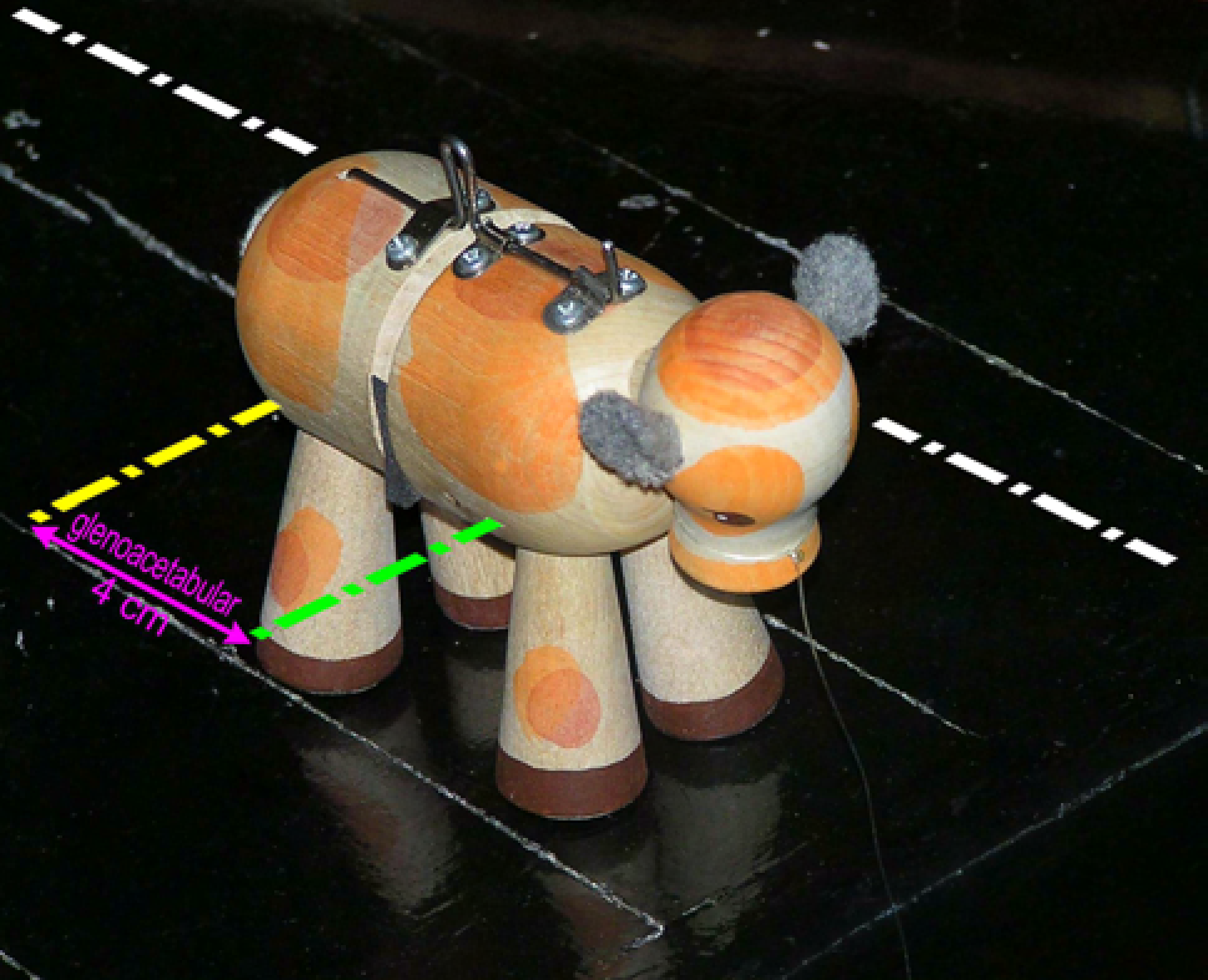

1
astragalus
fibula
V
tibia
I
2
I
tibia
V
fibula


60 cm
10 cm

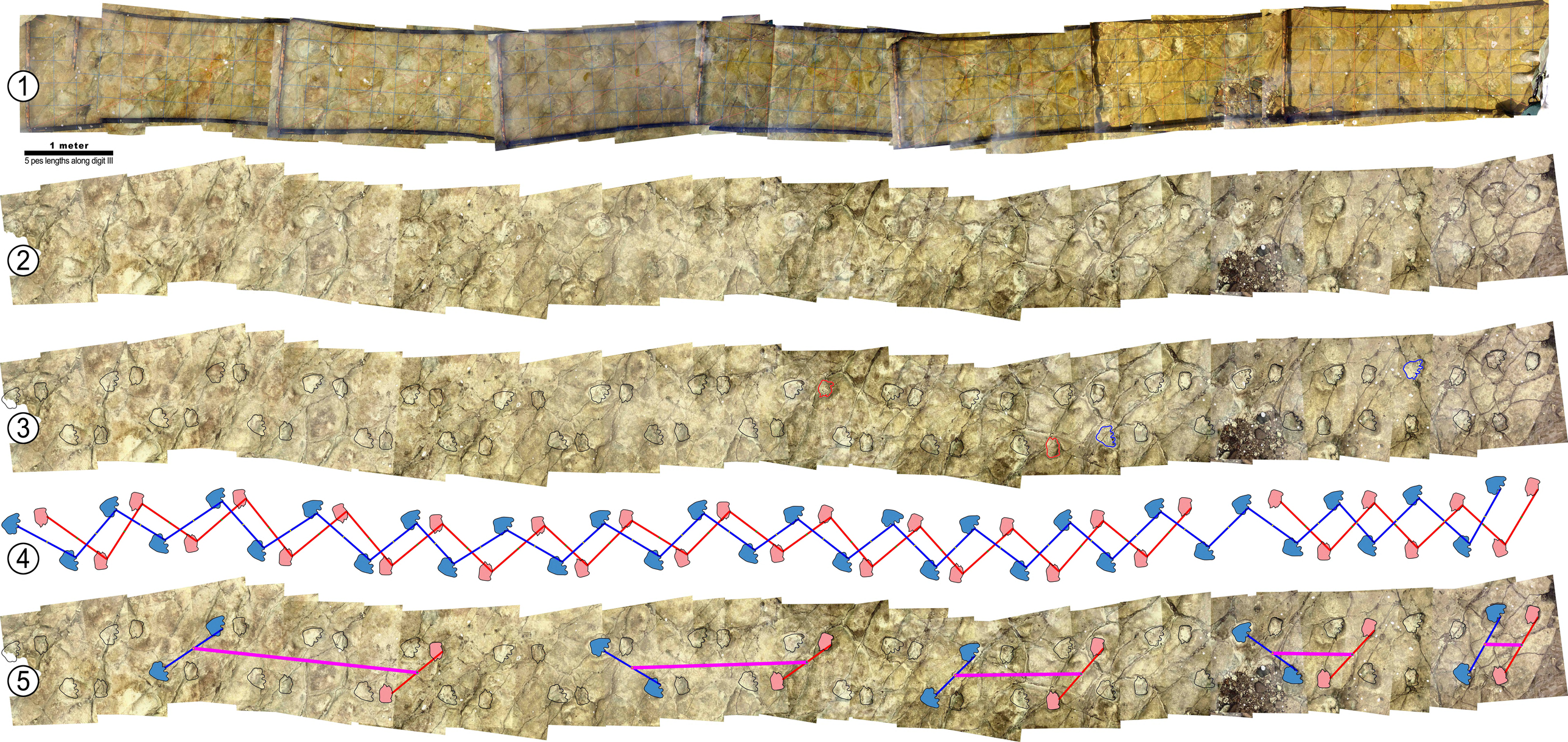

glenoacetabular
112 cm


V
I
average outline
radius
ulna


CoM
m. dorsalis scapulae
humerus
radius


glenoacetabular
4 cm




1
1 meter
5 pes lengths along digit III
2
3
4
5